Structure and Metamorphism in the Mono Craters Quadrangle Sierra Nevada, California

By RONALD W. KISTLER

CONTRIBUTIONS TO GENERAL GEOLOGY

GEOLOGICAL SURVEY BULLETIN 1221-E

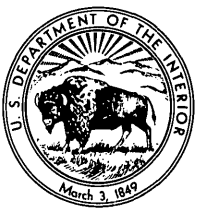

UNITED STATES GOVERNMENT PRINTING OFFICE, WASHINGTON : 1966

UNITED STATES DEPARTMENT OF THE INTERIOR

STEWART L. UDALL, *Secretary*

GEOLOGICAL SURVEY

William T. Pecora, *Director*

For sale by the Superintendent of Documents, U.S. Government Printing Office
Washington, D.C. 20402 - Price 50 cents (paper cover)

CONTENTS

ILLUSTRATIONS

TABLES

CONTRIBUTIONS TO GENERAL GEOLOGY

STRUCTURE AND METAMORPHISM IN THE MONO CRATERS QUADRANGLE, SIERRA NEVADA, CALIFORNIA

By RONALD W. KISTLER

ABSTRACT

The Mono Craters quadrangle, California, was an area of marine sedimentation during most of the Paleozoic. Rocks of Devonian and Mississippian ages have not been identified and may be absent; such a hiatus would suggest that the area was structurally high during the Antler orogeny, which affected rocks to the northeast in Nevada.

Marine miogeosynclinal sedimentary rocks of Ordovician(?), Silurian(?), Pennsylvanian(?), and Permian(?) age, called the Lewis sequence, were tightly folded along north-striking axial surfaces during a Permian(?) deformation tentatively correlated with the Sonoma orogeny of the same age in Nevada.

Volcanic and clastic sedimentary rocks, called the Koip sequence, were deposited in the Late Permian(?) unconformably on the folded Lewis sequence immediately after the Sonoman deformation. Both the Lewis and the Koip sequences were subsequently folded during a deformation that occurred in the Early or Middle Triassic. Axial surfaces of folds formed in this deformation strike northwest and are vertical or steeply dipping. A sequence of granodiorite and quartz monzonite plutons was intruded into the Permian(?) and older layered rocks in the Late Triassic and Early Jurassic, perhaps during the waning stages of this orogeny.

Coarse clastic sedimentary rocks and volcanic rocks, called the Dana sequence, were deposited in the Early Jurassic unconformably on the Koip sequence. The Lower Jurassic and older rocks were all folded during the Nevadan orogeny of Late Jurassic age.

A pluton of granodiorite, one of a sequence of plutons in the central Sierra Nevada, was intruded into the area of the quadrangle during the Late Cretaceous.

The effects of all three deformations are of regional extent and have been observed in the wallrocks and other roof pendants of the Sierra Nevada. The large-scale structures in the intruded pendant rocks could not be related to contacts with plutons. With the exception of the hornblende-bearing quartz monzonite in the east-central part of the quadrangle, the plutons were evidently emplaced passively.

Mineral assemblages in the roof pendants are the result of a complex metamorphic history and are compatible with the hornblende hornfels facies of contact metamorphism and the almandine amphibolite facies of regional metamorphism.

The Cenozoic history of the quadrangle is one of uplift and erosion. It is not well defined until the glacial advances and the volcanism in the pleistocene. Most of the faulting along the front of the Sierra Nevada in the quadrangle took place during the Pleistocene in the interval between the Sherwin Glaciation and the eruption of the Bishop Tuff. Since eruption of the Bishop Tuff, a maximum of 2,800 feet of displacement has occurred under Mono Lake along faults to the east of those along the range front.

INTRODUCTION

The Mono Craters 15-minute quadrangle in east-central California includes parts of the Basin and Range and Sierra Nevada physiographic provinces (fig. 1). Several thousand feet of the more than 6,500 feet of topographic relief in the area is due to displacement along faults that separate the two provinces. The crest of the Sierra Nevada is a sinuous line near the west boundary of the mapped area. Stream drainage is eastward from this crest into Mono Lake Basin and westward into the Tuolumne River.

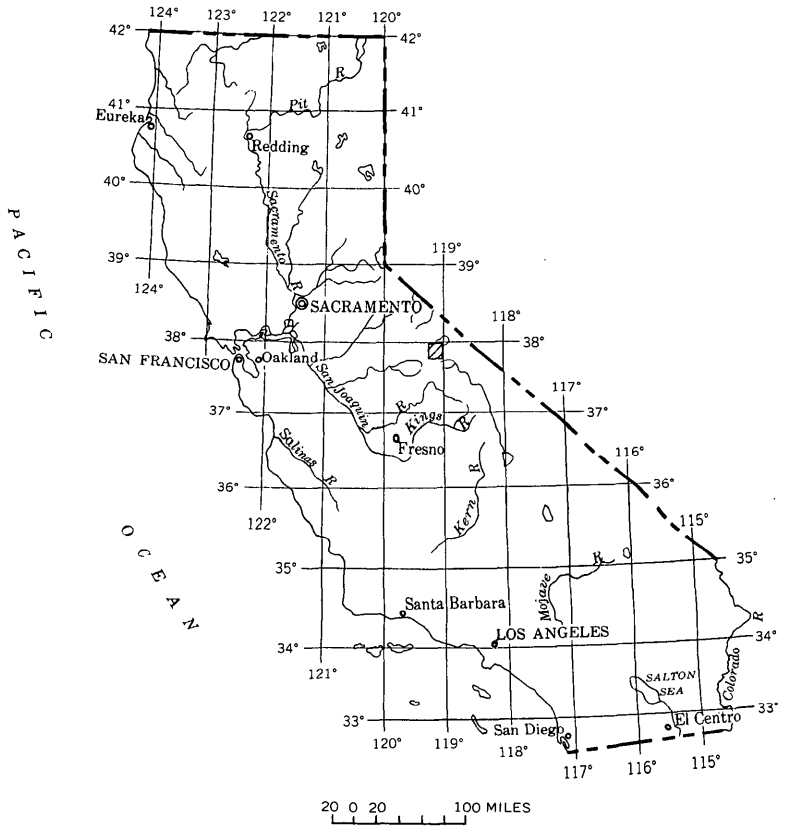

FIGURE 1.—Location of Mono Craters quadrangle.

Metamorphosed Paleozoic and Mesozoic sedimentary and volcanic rocks and Mesozoic granitic rocks compose the basement complex of the area. Within the granitic rocks are roof pendants of metamorphic rocks that were complexly deformed during at least three tectonic episodes prior to the last phase of plutonic activity. The textures and mineral assemblages formed during metamorphism are compatible with the hornblende hornfels facies and (or) the almandine amphibolite facies. The granitic rock, mostly granodiorite or quartz monzonite, occurs in plutons of moderate size.

Tertiary or Quaternary volcanic rocks and Quaternary lake sediments, moraines, pumice deposits, and alluvium cover the basement complex in the Mono Basin and in part of the Sierra Nevada.

The Mono Craters quadrangle map (1:62,500) was photographically enlarged to 1:48,000 as a base for geologic mapping. Selected areas of this map were photographically enlarged (1 in. = 1,000 ft.) to permit detailed mapping in parts of the structurally complex roof pendants.

PREVIOUS GEOLOGIC INVESTIGATIONS

Whitney (1865) described the islands in Mono Lake and the volcanic domes in the vicinity. LeConte (1879) wrote about the relation of the Mono Craters to the glacial drift. Russell (1889) discussed the physiography and the general geology of the region and was the first observer to recognize multiple glaciation there.

The exposures of moraines extending from canyons incised in the Sierra scarp have attracted geologists to the region (Matthes, 1930; Blackwelder, 1931). The Tioga Glaciation was named by Blackwelder for glaciers that existed in Tioga Pass. Kesseli (1939) and Putnam (1949) studied the origin of Reversed Creek in the southern part of the quadrangle and the general Quaternary history of the region. Cloos (1936), Balk (1937), and Mayo (1941) considered the problem of granite tectonics in part of the quadrangle and in areas to the west and south. Williams (1932), Gilbert (1938), and Putnam (1938) published accounts of the volcanic rocks found in the eastern part of the quadrangle. Dunn (1950) mapped the northern part of the quadrangle and the rocks in the immediate vicinity to the north. Rose (1957) described the granitic rocks in the northwestern part of the quadrangle. Pakiser and others (1960) presented data and conclusions derived from extensive geophysical work in the Mono Basin.

The following authors have published accounts of the regional geologic framework of the Mono Craters area: Rinehart and Ross (1957, 1964); Bateman and others (1963); Moore (1963); Huber and Rinehart (1965); and Kistler (1966).

219-260 O—66——2

SCOPE OF REPORT AND ACKNOWLEDGMENTS

This report describes the deformational history of the metamorphic rocks in the roof pendants and the faulting along the Sierra Nevada front in the Mono Craters quadrangle. This deformational history is compared to that of rocks of similar age in the ranges of western Nevada and in other roof pendants in the central Sierra Nevada. The relation of deformation to plutonism in the area is also discussed.

The initial part of the study was done under the auspices of the University of California at Berkeley (Kistler, 1960). That part of the study benefited from the guidance and suggestions of Dr. G. H. Curtis, and the review by Dr. Curtis, Dr. L. E. Weiss, and Prof. Edward Wisser.

Through further fieldwork, with the U.S. Geological Survey, details have been added to the intial geologic map, and the ideas presented in the intial report have been strengthened.

METAMORPHIC ROCKS

STRATIGRAPHY AND STRUCTURE

The metamorphic rocks occur as discontinuous roof pendants in a complex of granitic plutons. The largest metamorphic body, about 3 miles wide and 10 miles long, is the northern extension of the Ritter Range pendant (Rinehart and others, 1959; Huber and Rinehart, 1965; Kistler, 1966). The other major metamorphic bodies in the quadrangle are the Gull Lake roof pendant, the Log Cabin Mine roof pendant, and the south end of the Saddlebag Lake roof pendant (fig. 2).

Two angular unconformities in the metamorphic rocks are manifested by (1) increasing complexity of folding in successively older rock units; (2) presence of conglomerates locally on Mount Dana; and (3) marked changes in lithologies of successive rock units, indicating changes in depositional environment of the rocks. In accord with the terminology of Silberling and Roberts (1962, p. 6), the two unconformities were used to mark the boundaries of three rock "sequences," here informally termed, in order of decreasing age, the "Lewis sequence," the "Koip sequence," and the "Dana sequence."

The base of the Lewis sequence is unknown, but the basal units of both the Koip and Dana sequences, observed on Mount Dana, are conglomerates (fig. 3). At exposures of metamorphic rock in the Ritter Range pendant, where the Koip sequence is in depositional contact with the underlying Lewis sequence, the conglomerate at the base of the Koip sequence is absent. Truncated beds in the relatively older units at the unconformities, although looked for, were not observed.

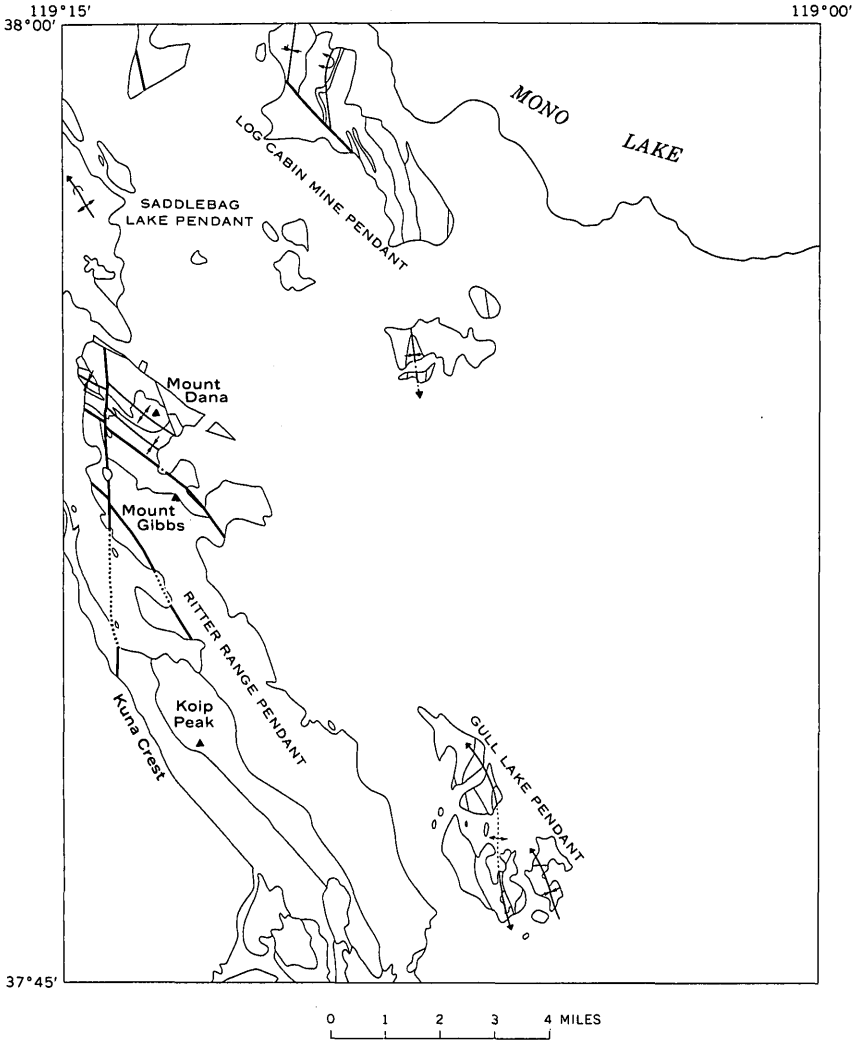

FIGURE 2.—Location of roof pendants in the Mono Craters quadrangle.

The Lewis sequence has at least three generations of folds; the Koip sequence, two generations; and the Dana sequence, one generation.

The three sequences are separated into informal lithologic units in table 1. Fossils tentatively identified as crinoid stems were found in two units of the Lewis sequence—one unit is in the Log Cabin Mine roof pendant, and the other, in the Gull Lake roof pendant. The Lewis, Koip, and Dana sequences are assigned to the Paleozoic, Upper Permian(?), and Lower Jurassic, respectively, on the basis of lithologic correlations, stratigraphic succession, and isotopic age determinations.

FIGURE 3.—Conglomerate at base of the Koip sequence. Tectonically flattened cobbles and pebbles of conglomerate are composed mostly of quartzite and quartzofeldspathic hornfels, whereas aluminous matrix of rock is pelitic hornfels. Outcrop is at confluence of uppermost tributaries of Dana Fork Tuolumne River, on south flank of Mount Dana.

The Paleozic rocks of the Lewis sequence occur in all major roof pendants in the quadrangle and occupy about 20 square miles (fig. 4). These metamorphosed sedimentary rocks are the reconstituted equivalents of siltstone, mudstone, impure quartz sandstone, impure limestone, chert, and conglomerate. The tops of beds can be recognized by scarce relict sedimentary structures such as crossbedding, graded bedding, and channel fillings. These features, in addition to minor overturned folds, indicate that the bedding is in places overturned eastward.

Three generations of folds can be recognized in the Lewis sequence. Two synclines and an overturned anticline large enough to be shown on the map (pl. 1) occur in the Log Cabin Mine pendant. These

folds (fig. 5) have axial surfaces that strike north; the axial surfaces of two folds are vertical, and that of the other fold dips about 45° W. Folds of this generation do not occur in the Koip and Dana sequences; relations to other folds indicate that these were the first to be formed in the metamorphic rock. The principal fold in the Gull Lake pendant, of the same generation as those observed in the Log Cabin Mine pendant, is an anticline that plunges steeply to the southeast. The original orientation of this fold was altered to its present attitude by later deformation.

TABLE 1.—*Lithologic units in the sequences in roof pendants, Mono Craters quadrangle*

		Ritter Range pendant	Saddlebag Lake pendant	Gull Lake pendant	Log Cabin Mine pendant
Dana sequence	Lower Jurassic	Graywackes, volcanic tuffs and flows, crossbedded sandstones. Marble and calc-silicate hornfels. Volcanic tuffs and flows, lapilli-tuff shale, calc-silicate hornfels. Basal conglomerate			
Koip sequence	Upper Permian(?)	Quartzofeldspathic hornfels, calc-silicate hornfels, volcanic flows. Andesite flows and breccias, local graywacke and sandstone lenses. Acid volcanic tuffs, volcanic flows, local graywackes. Local basal conglomerate.			
Lewis sequence	Permian(?)	Quartzofeldspathic hornfels, calc-silicate hornfels, carbonaceous marbles.	Quartzofeldspathic hornfels, calc-silicate hornfels.	Quartzofeldspathic hornfels.	
	Pennsylvanian(?) and Permian(?)			Carbonaceous marble. Calc-silicate hornfels, quartzite, quartzofeldspathic hornfels. Marble calc-silicate hornfels.	
	Ordovician(?) and Silurian(?)				Marble and calc-silicate hornfels. Biotite-bearing quartzite. Andalusite hornfels, quartzofeldspathic hornfels, carbonaceous marbles, crossbedded calcareous quartzite. Marble, calc-silicate hornfels, quartzite. Quartzofeldspathic hornfels. Marble, calc-silicate hornfels.

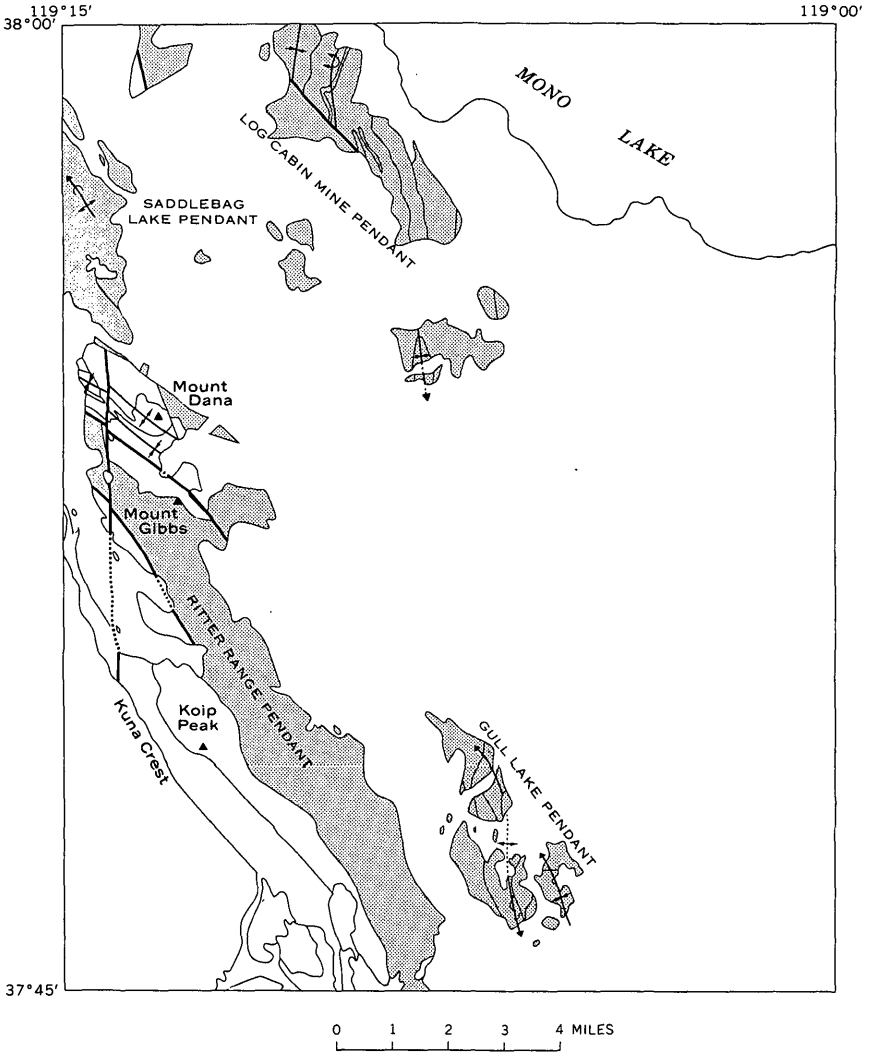

FIGURE 4.—Outcrops of the Lewis sequence in roof pendants, Mono Craters quadrangle.

Crests of two northwest-plunging folds that formed in a later deformation occur along the east boundary of the Gull Lake pendant.

In the Ritter Range pendant, folds of map-scale extent in the Lewis sequence were not determined, owing to the lack of distinctive lithologic units. However, a complex anticline that plunges moderately to the northwest is defined on the map in these same units in the Saddlebag Lake roof pendant.

Small folds and lineations characterize the Lewis sequence (figs. 5, 6, and 7), and many folds that are too small to be shown on the map

FIGURE 5.—Tight folding in thin-bedded metamorphosed siltstone in the Lewis sequence, Log Cabin Mine roof pendant. Axial planes of these folds virtually parallel bedding, which here strikes about north and dips 45° W. View is to the south.

FIGURE 6.—Minor folds in a calc-silicate hornfels in the Lewis sequence, Gull Lake roof pendant.

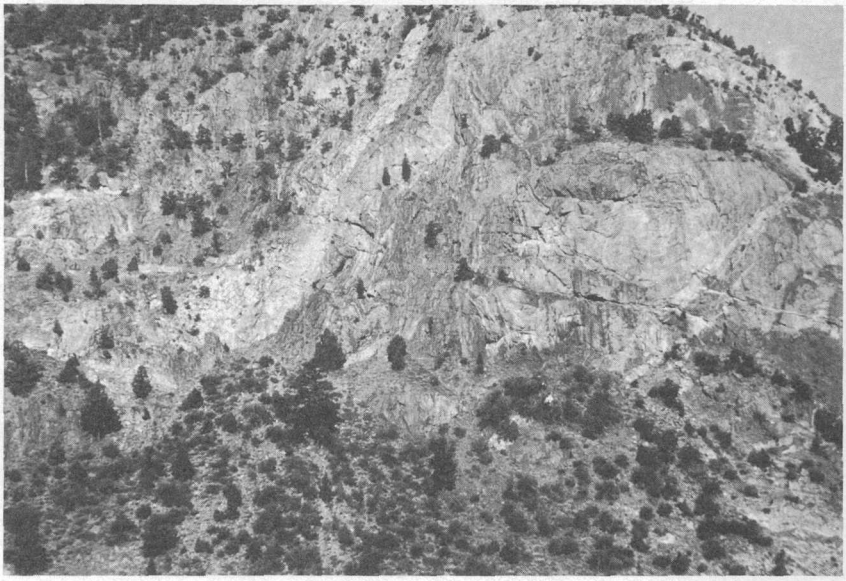

FIGURE 7.—Folds in the Lewis sequence, Gull Lake roof pendant.

were observed or determined by indirect methods. Axial-plane cleavages are well developed in schistose rocks, and in places these cleavages replace the bedding as the dominant planar surface. The dominant cleavages are the same as those observed in the Koip sequence, and each set is related to a specific fold system.

The Lewis sequence closely resembles, and is believed to be correlative with, a fossiliferous sequence of Ordovician, Silurian(?), Pennsylvanian, and Permian(?) strata in the Mount Morrisson roof pendant, about 15 miles to the southeast (Rinehart and Ross, 1964). In the northern extension of the Ritter Range pendant, rocks of the Lewis sequence lie unconformably below, and in depositional contact with, the foliated volcanic rocks of Permian(?) age in the Koip sequence. They have the same stratigraphic position and lithology as the Permian(?) Bloody Mountain Formation in the Mount Morrison pendant (Rinehart and Ross, 1964, p. 26–27). The rocks at the south end of the Saddlebag roof pendant are lithologically similar to the rocks of the Lewis sequence in the Ritter Range pendant and are therefore also considered to be Permian(?). In the Gull Lake pendant the quartzofeldspathic hornfels unit, the calc-silicate hornfels, quartzsite, and quartzofeldspathic hornfels unit, and the marble and calc-silicate hornfels unit (Kistler, 1966) occur in the same order as the lithologically similar Bloody Mountain Formation, Lake Dorothy and Mildred Lake Hornfelses, and Mount Baldwin Marble (Rinehart

and Ross, 1964, p. 24–27), respectively. The rocks of the Gull Lake pendant are therefore assigned to the Pennsylvanian(?) and Permian(?). In the Log Cabin Mine roof pendant the dominant rock types are marble, andalusite hornfels and chiastolite shale, calcareous sandstone, and chert. These lithologies are similar to those of the Convict Lake and McGee Mountain blocks of the Mount Morrison pendant (Rinehart and Ross, 1964, p. 17–23). Two measured sections of the rocks in the Log Cabin Mine roof pendant (located in fig. 8) are given in table 2. The lithologies, which are similar to those of Ordovician and Silurian(?) rocks of the Mount Morrison pendant (Rinehart and Ross, 1964, p. 11), permit tentative assignment of the rocks in the Log Cabin Mine pendant to the Ordovician(?) and Silurian(?).

Rocks of the Koip sequence crop out in an area of about 10 square miles on Mount Dana and Mount Gibbs and along the west boundary of the Ritter Range pendant (fig. 9). These rocks are predominantly the reconstituted equivalents of rhyolitic pyroclastic rocks, andesite and dacite flows, and minor basalts. Interbedded impure quartz sandstones and impure limestones are common near the top of the sequence. Coarsely crystalline lithic wackes occur throughout the section and in places exhibit graded bedding. Bedding has been disrupted in places and now occurs as a compositional banding of lens-shaped layers that define a foliation parallel to bedding. The rocks dip steeply, and some large complex folds were observed (figs. 10, 11). A northwest-trending syncline (of mappable scale) plunges beneath the unconformably overlying Dana sequence on Mount Dana. Preferred orientation of mica defines cleavages that are parallel to the axial surfaces of the two generations of folds in the sequence. One cleavage is vertical and strikes about N. 30° W. (fig. 12); the other dips steeply and strikes about N. 50° W., parallel to the axial surfaces of younger folds (fig. 13) that intersect and deform folds of the type shown in figure 12. Lineations observed are lines at the intersections of bedding and cleavage (fig. 14) and elongate pebbles (fig. 15). The lineations are parallel to minor-fold axes.

Analysis of five specimens from the Koip sequence by the rubidium-strontium whole-rock technique (C. E. Hedge, written commun., 1961) indicates a Permian(?) age (265 m.y.). Analytical data for the age determination are shown in figure 16. Lithologically the Koip sequence is similar to volcanic rocks of the Middle Triassic Excelsior Formation in Nevada and is also similar to Permian volcanic rocks of the Toyabe Range (Ferguson and Muller, 1949, p. 4–5). Volcanic rocks of the Excelsior Formation are assigned to the Middle Triassic on the basis of fossil evidence in the Gillis Range about 50 miles north-

TABLE 2.—*Lithologic sections in the Lewis sequence, Log Cabin Mine roof pendant, showing altitudes along lines A–A′ and B–B′ of figure 8*

Altitude (ft)	*Lithologic section*
	A–A′
9,600	Buff siliceous hornfels.
	Siliceous shale and black quartzite.
	Calc-silicate hornfels.
	Gray andalusite hornfels.
9,580	Light-gray siliceous hornfels.
9,500	Green siliceous hornfels.
9,410	Green calc-silicate hornfels.
	Buff-brown mudstone.
9,360	Gray siliceous hornfels.
9,300	Black calcareous shale.
9,250	Green calc-silicate hornfels.
	Gray andalusite shale.
	Black siliceous hornfels.
9,040	Fissile black siliceous shale.
	Buff-gray calc-silicate hornfels.
9,000	Black siliceous shale.
	Gray sandy limestone.
	Buff and black siliceous hornfels.
	Black chiastolite shale.
	Gray calc-silicate hornfels.
	Black andalusite hornfels.
8,620	Black siliceous hornfels.
8,500	Black siliceous shale.
	Andalusite hornfels.
8,440	White and gray marble.
8,200	Black siliceous hornfels.
7,930	Gray siliceous hornfels.
	Gray marble.
7,760	Black siliceous hornfels.
	B–B′
9,360	Gray siliceous hornfels.
9,340	Black andalusite hornfels.
9,260	Black calcareous sandstone.
	Black shale.
9,200	Black sandy marble.
9,180	Crossbedded sandy limestone.
9,050	Purple siliceous shale.
8,960	Dark-gray limestone.
8,950	Crossbedded gray marble.
8,800	Black impure limestone.
8,780	Gray limestone and chert.
8,600	Black siliceous hornfels.
8,500	Black calcareous shale.

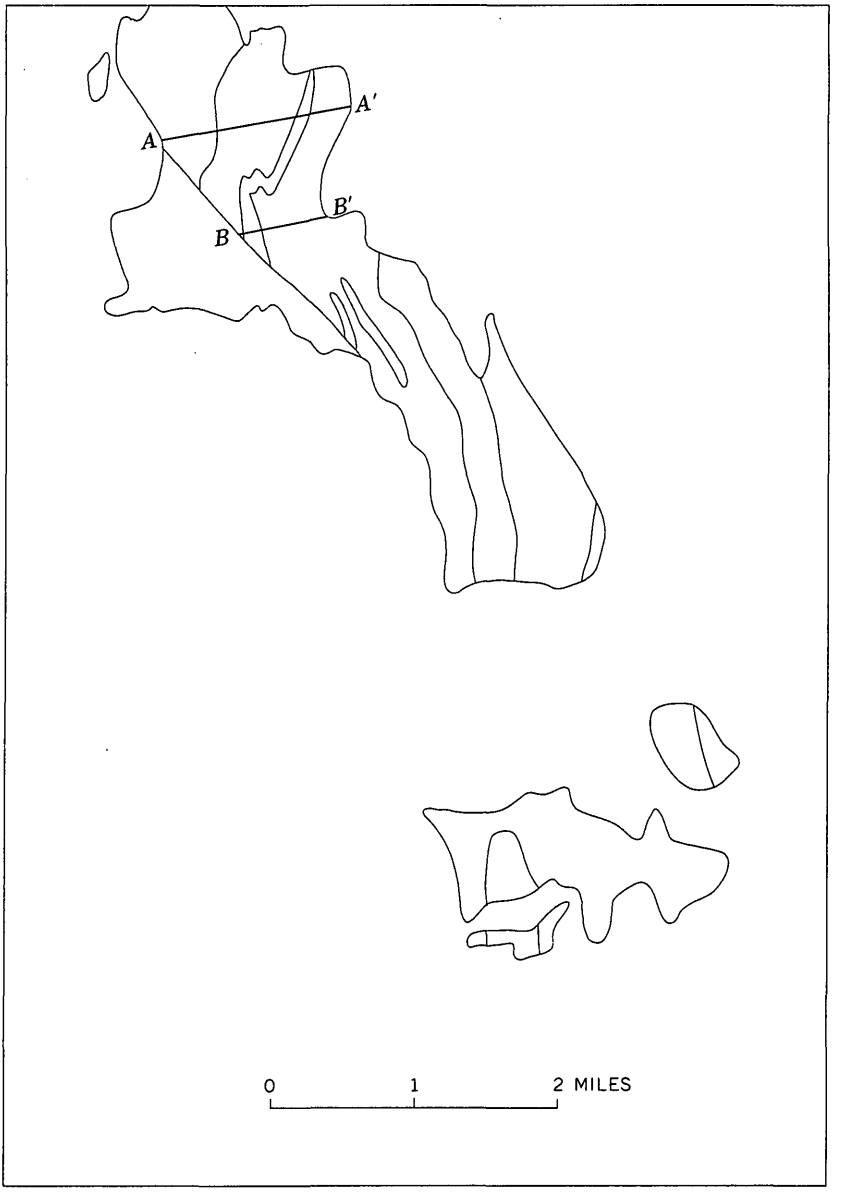

FIGURE 8.—Location of lithologic sections *A–A'* and *B–B'* Log Cabin Mine roof pendant. Altitudes along lines are given in table 2.

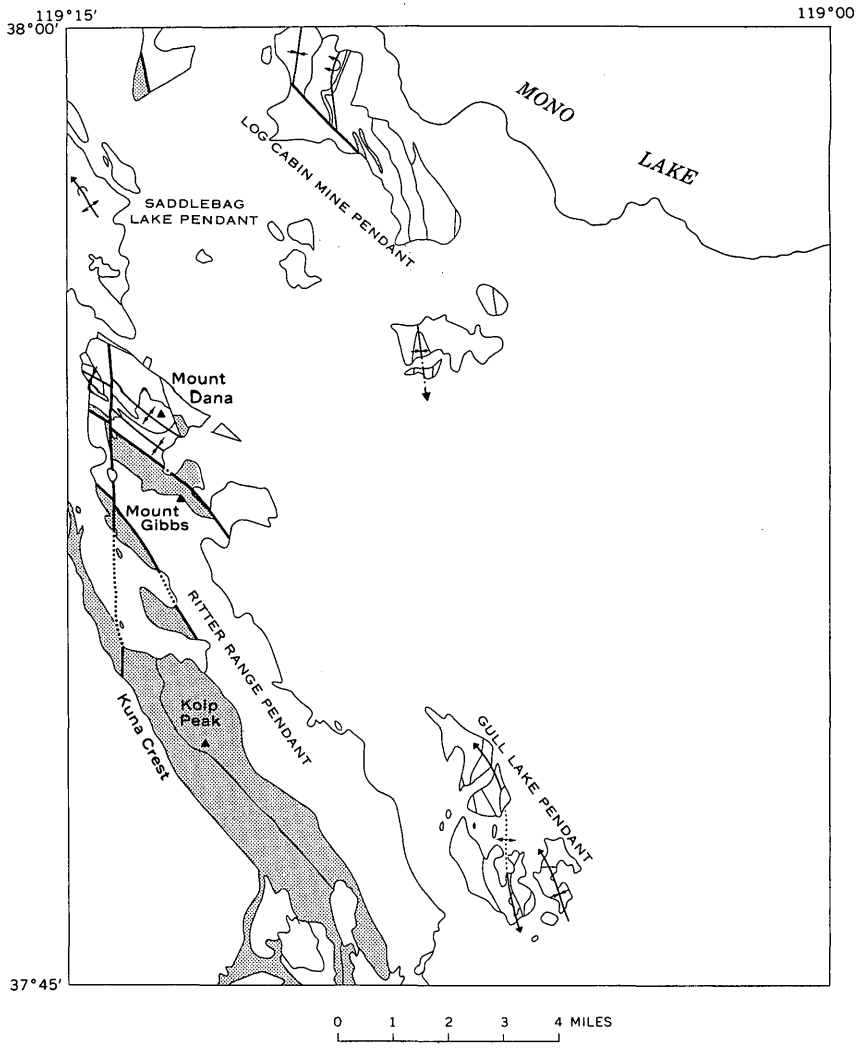

FIGURE 9.—Outcrops of the Koip sequence in roof pendants of the Mono Craters quadrangle.

FIGURE 10.—Steeply dipping metamorphosed graywackes and volcanic rocks of the Koip sequence on ridge by the Alger Lakes. View is to the southeast, from Koip Peak.

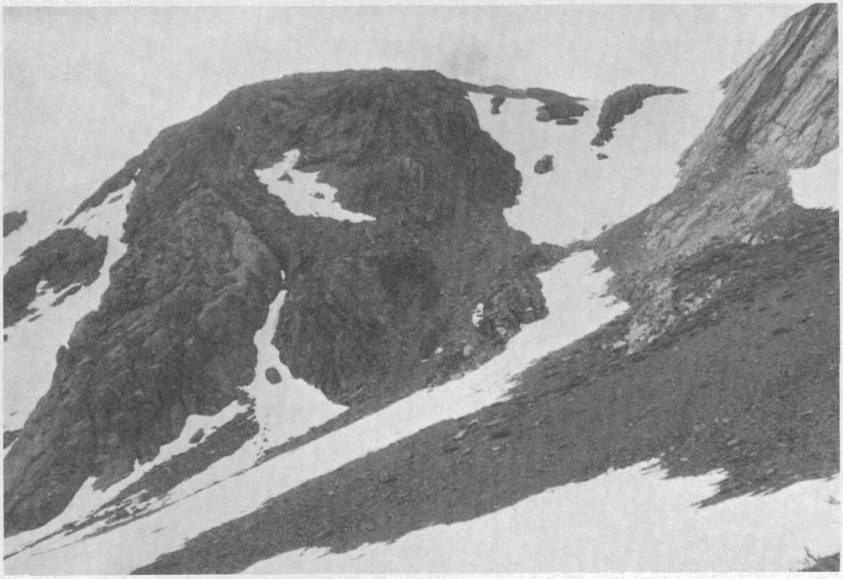

FIGURE 11.—Complex folding in metamorphosed graywackes and volcanic rocks of the Koip sequence on ridge south of Spillway Lake. View is to the south.

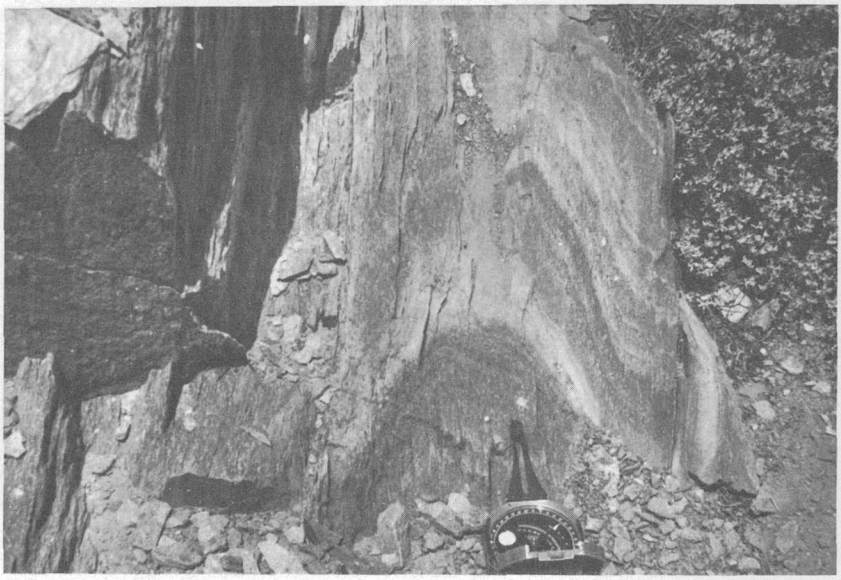

FIGURE 12.—Fold in volcanic phyllite in the Koip sequence. Axial-plane cleavage strikes about N. 30° W.

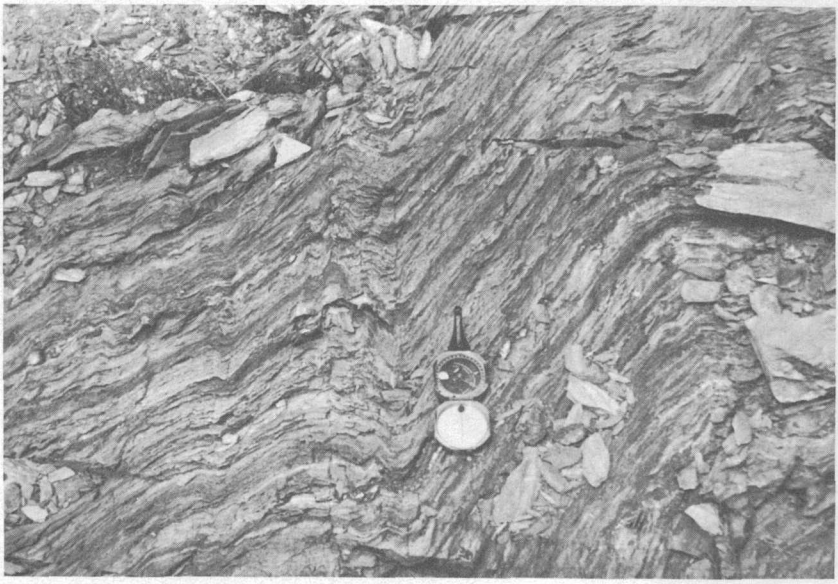

FIGURE 13.—Folds in foliated volcanic rock of the Koip sequence. Axial planes of folds are paralleled by cleavage that strikes about N. 50° W. and dips steeply to the northeast.

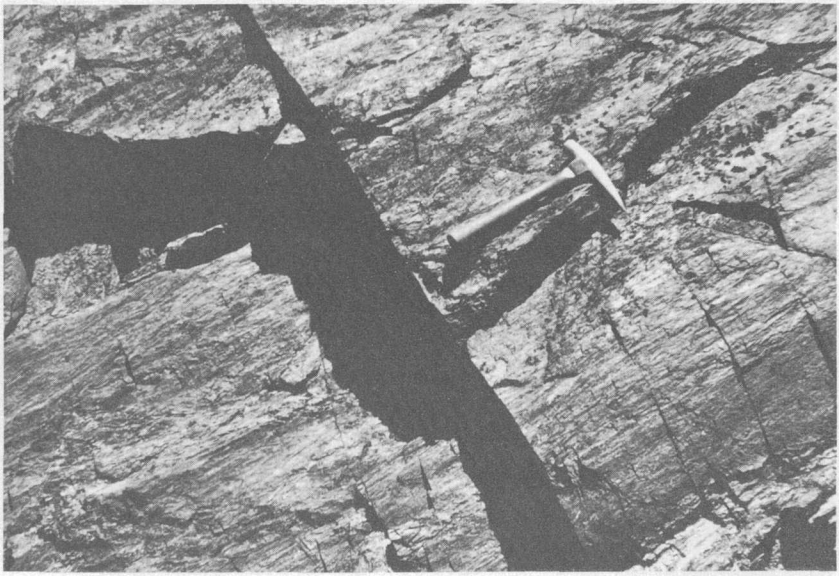

FIGURE 14.—Lineations caused by intersecting cleavage and bedding in metamorphosed volcanic rocks of the Koip sequence.

east of the Ritter Range. Ferguson and Muller (1949, p. 5), however, stated: "That the similar volcanic rocks in the nearby ranges are also of Middle Triassic age becomes less certain with increasing distance from the Gillis Range area." The Permian(?) age of the lithologically similar Koip sequence is consistent with this observation.

The Dana sequence lies unconformably on the Permian(?) Koip sequence and occupies the same stratigraphic position as fossiliferous Lower Jurassic sedimentary and volcanic rocks reported by Rinehart and others (1959) in the Ritter Range pendant to the south. The Dana sequence is lithologically similar to the Lower Jurassic Dunlap Formation of western Nevada, described by Ferguson and Muller (1949, p. 6) and, therefore, is assigned to the Lower Jurassic.

The principal rock types of the Dana sequence, which crops out in an area of about 3 square miles on Mount Dana (fig. 17), are subfeldspathic lithic wackes, volcanic flows and tuffs, and shales. Sandstone units commonly are crossbedded and exhibit scour and fill features (fig. 18). The cross laminae are so large that in small outcrops they can be mistaken for true bedding. Epidote is abundant, and outcrops are green in places. Beds dip gently to moderately throughout the sequence, and in the top 1,000 feet of Mount Dana, rarely dip more than 25° (fig. 19). Gently dipping beds at the top of Mount Dana lie in the crest of a northwest-trending anticline that has a subhorizon-

tal axis. Steeper dips occur in the southwest limb of the adjoining syncline on the south flank of the mountain (fig. 20). Minor folds, seldom observed, have horizontal or gently plunging axes and vertical axial surfaces that strike about N. 50° W. Cleavage parallel to the axial surfaces of folds is shown in the shales and calcareous rocks by the parallel arrangement of micas but is generally absent from coarser grained rocks, such as sandstone. Northwest-trending faults parallel the axial surfaces of folds and reflect extreme strain during the deformation that produced folding.

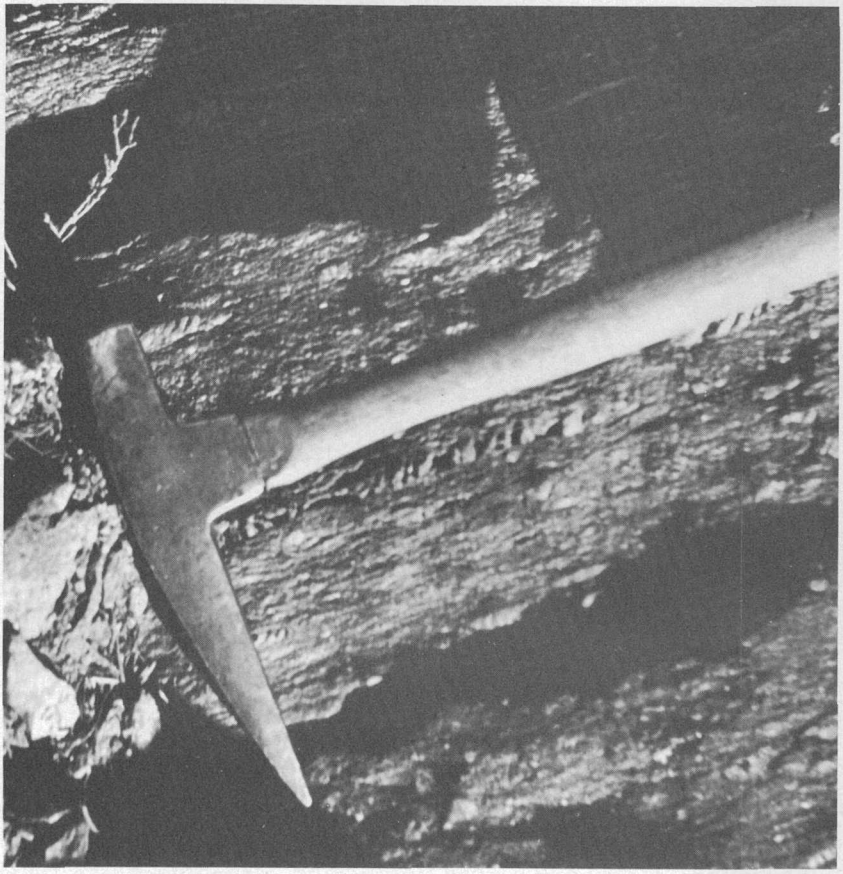

FIGURE 15.—Tectonically elongated pebbles in volcanic wacke in the Koip sequence.

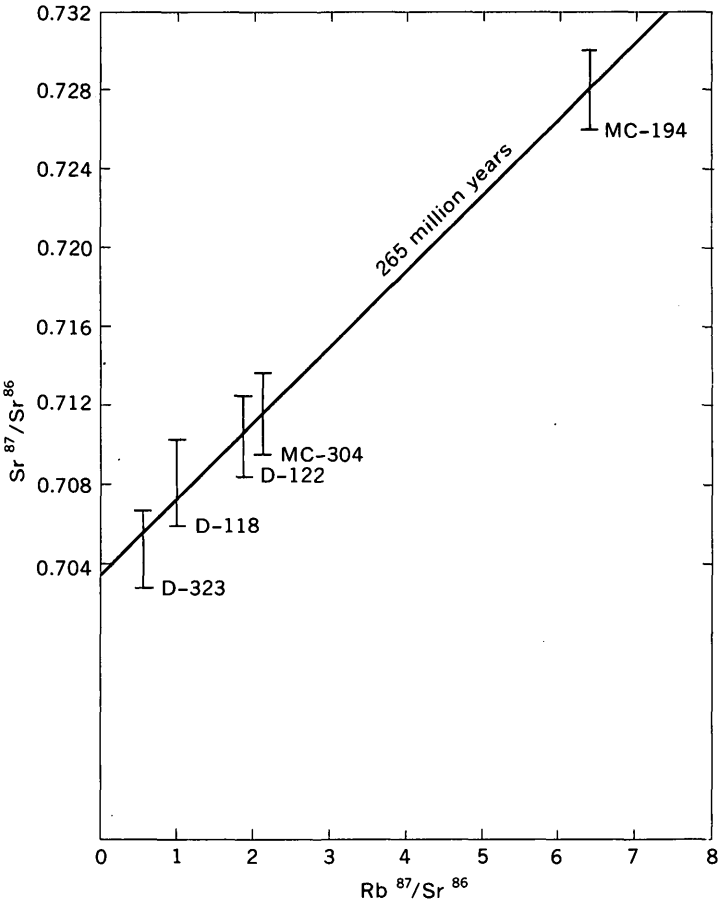

Sample	Rb (ppm)	Sr† (ppm)	Sr^{87}/Sr^{86}*	Rb^{87}/Sr^{86}
D-323	72.4	464	0.7046	0.456
D-118	100	320	.7081	.915
MC-304	120	173	.7116	2.02
D-122	128	207	.7105	1.81
MC-194	282	131	.7281	6.26

†Normal strontium.
*Unspiked—normalized to an 86/88 ratio of 0.1194.

FIGURE 16.—Analytical data and rubidium-strontium isochron age determinations for specimens of the Koip sequence. 0.283 g Rb^{87} per g Rb; rubidium decay constant, $\lambda\beta = 1.47 \times 10^{-11}$ $year^{-1}$.

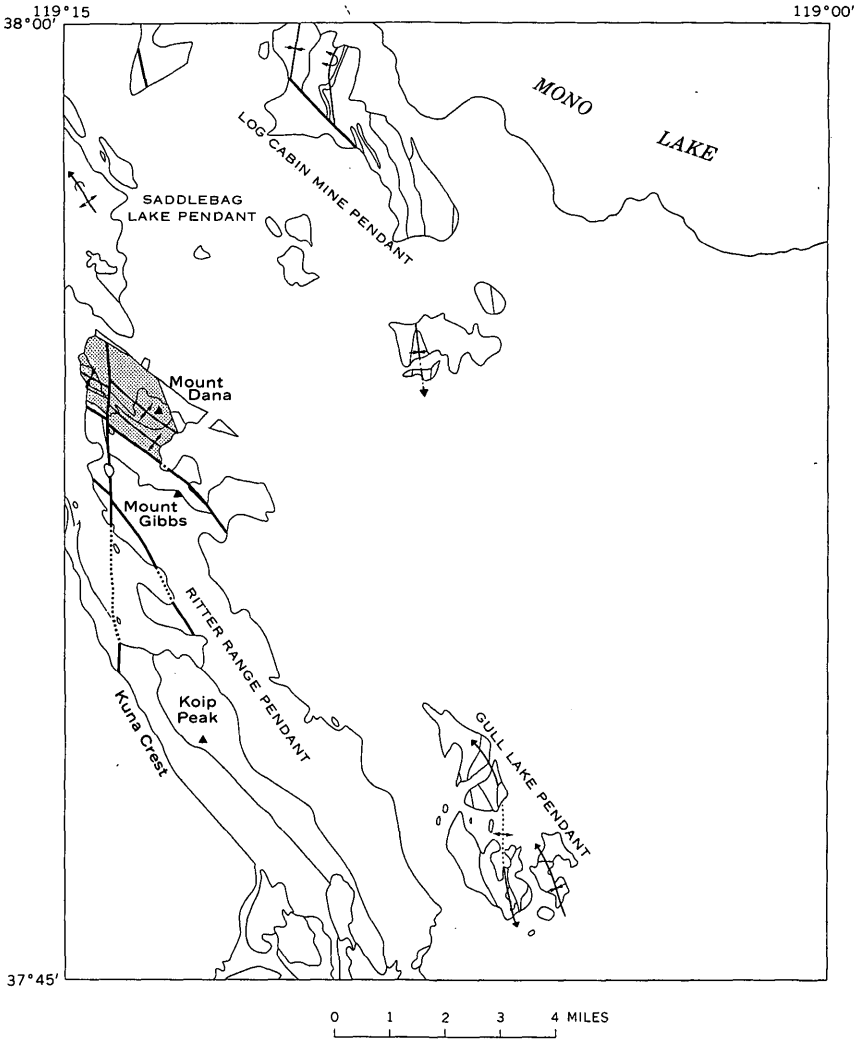

FIGURE 17.—Outcrop of the Dana sequence in Ritter Range roof pendant, Mono Craters quadrangle.

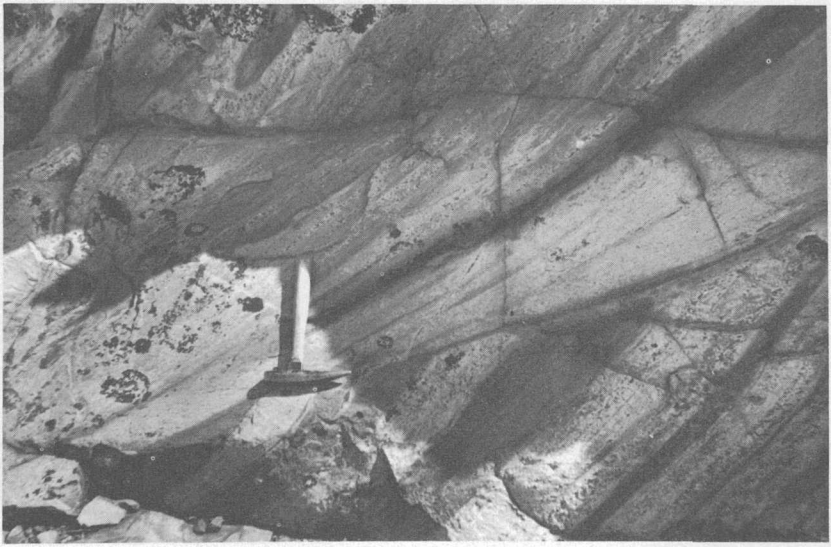

FIGURE 18.—Scour and fill in sandstone unit of the Dana sequence. Outcrop is on west flank of Mount Dana.

FIGURE 19.—Bedding in the Dana sequence at top of Mount Dana. View is south from Dana Plateau.

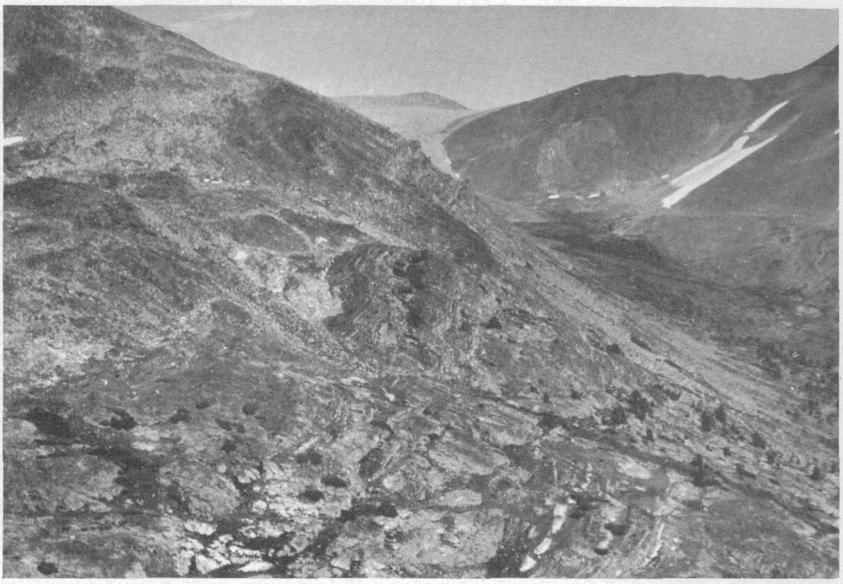

FIGURE 20.—Bedding in the Dana sequence on southwest flank of Mount Dana. View is to east, from west flank of mountain.

PETROGRAPHY

METAMORPHIC ASSEMBLAGES

Most of the roof pendants are composed of metamorphic derivatives of pelitic, quartzofeldspathic, calcareous, and mafic rocks. Quartzofeldspathic assemblages predominate and occur in each rock sequence. Pelitic rocks made up about a quarter of the Log Cabin Mine roof pendant, but they are sparse in other pendants. Calcareous rocks occur in all the sequences, but they are most common in the Lewis sequence in the Gull Lake and Log Cabin Mine roof pendants. Mafic rocks, mostly derivatives of basalt and andesite flows, are restricted to the Koip and Dana sequences. Mineral paragenesis in the roof pendants, determined by petrographic examination of 150 thin sections, is summarized in table 3. The mineralogy at each specimen locality is shown on plate 2.

The metamorphic assemblages can be divided into two groups that probably represent different pressures and, possibly, different temperatures during metamorphism. The mineral assemblages of the first group are compatible with the hornblende-hornfels facies (Fyfe and others, 1958, p. 205–211) and are characterized by the presence of wollastonite in calcareous assemblages and andalusite in pelitic assemblages. The mineral assemblages of the second group are com-

TABLE 3.—*Summary of mineralogy of the metamorphic rocks in the Mono Craters quadrangle*

[MC, major constituent; mc, minor constituent; --, absent]

Mineral	Dana sequence	Koip sequence	Lewis sequence		
			Ritter Range roof pendant	Gull Lake roof pendant	Log Cabin Mine roof pendant
Quartz	MC	MC	MC	MC	MC.
Plagioclase	MC	MC	MC	MC	--
K-feldspar	MC	MC	--	MC	mc.
Biotite	MC	MC	MC	mc	MC.
White mica	mc	MC	Trace	mc	MC.
Andalusite	--	Trace	Trace	--	MC.
Amphibole [1]	MC	MC	MC	MC	MC.
Clinopyroxene	mc	Trace	Trace	MC	MC.
Pistacite	MC	Trace	Trace	mc	--
Clinozoisite	Trace	mc	mc	Trace	mc.
Zoisite	--	Trace	--	Trace	Trace.
Calcite	Trace	mc	mc	mc	MC.
Garnet	Trace	mc	Trace	mc	mc.
Idocrase	--	--	Trace	Trace	Trace.
Wollastonite	--	--	--	MC	MC.
Scapolite	Trace	--	--	--	--
Cordierite	Trace	--	--	--	--
Tourmaline	--	mc	--	Trace	--
Chlorite	--	Trace	--	Trace	Trace.
Lithic fragment	mc	mc	--	--	--
Chert	--	--	--	--	Trace.

[1] Questionable cummingtonite and anthophyllite in Log Cabin Mine pendant.

patible with the almandine-amphibolite facies (Fyfe and others, 1958, p. 228–232) and are characterized by the presence of calcite and quartz in calcareous assemblages. Also, plagioclase more calcic than albite occurs with epidote in the second group. The rocks of the Log Cabin Mine roof pendant are metamorphosed to the hornblende-hornfels facies, whereas rocks of the other roof pendants are metamorphosed to the almandine-amphibolite facies and (or) the hornblende-hornfels facies.

TEXTURES

Most rock textures of the Lewis and Koip sequences are granoblastic, but the shales and some volcanic rocks are schistose. Sedimentary textures are preserved in most of the coarser sandstones, particularly in those of the Dana sequence. Blastoporphyritic and blastophitic textures identify, respectively, metamorphosed volcanic flows and tuffs, and diabase intrusions. Many micaceous schists in the Lewis and Koip sequences have two distinct planar preferred orientations of mica. Skarns adjacent to intrusive contacts are generally coarse

grained, and in some, large crystals of wollastonite poikiloblastically enclose euhedral granular crystals of diopside. Photomicrographs of typical textures in the metamorphic rocks are shown in figures 21–26.

MINERALOGY

Quartz is present in all metamorphic assemblages except some derivatives of basic volcanic rocks and a few skarns. Feldspar, mica, amphibole, epidote, clinopyroxene, wollastonite, calcite, andalusite, and garnet are the major minerals in the metamorphic assemblages.

Quartz.—Generally quartz occurs in sandstone as a fine-grained granoblastic inclusion-crowded mosaic and is recrystallized. Quartz may retain angular outlines in the coarser sandstones where it is obviously detrital. In metamorphic rhyolites, embayed subhedral relict phenocrysts of quartz occur with fine anhedral quartz associated with fine anhedra of alkalic feldspar in the rock matrix. In hornfels, quartz occurs as a fine mosaic of anhedral crystals.

Feldspar.—Plagioclase determinations were made by universal stage, using the methods described by Turner (1947), and by measurement of extinction angles of sections normal to principal optical

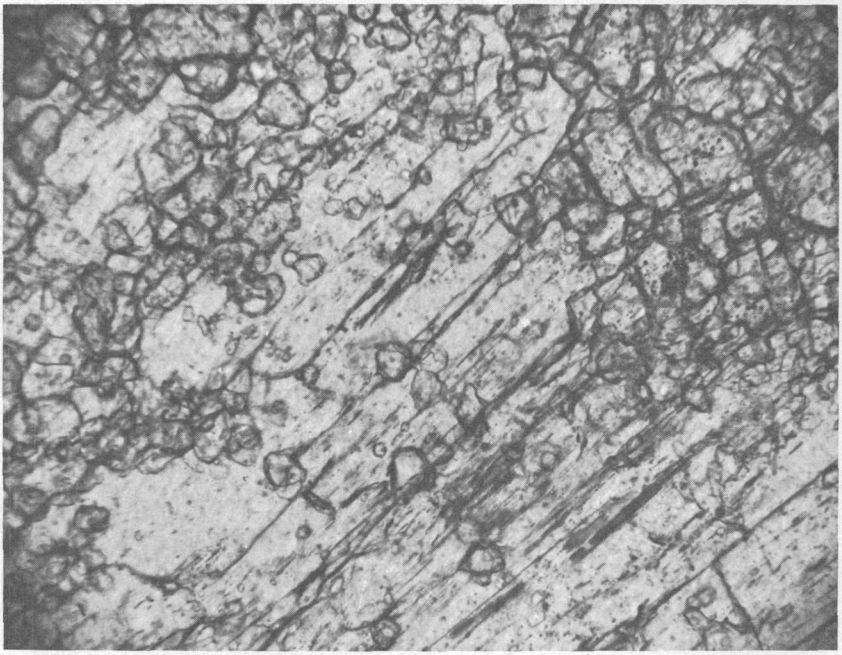

FIGURE 21.—Wollastonite skarn. Granular colorless diopside is poikiloblastically enclosed in wollastonite. × 94. Lewis sequence.

planes as described by Tröger (1956, p. 101). Small grain sizes and (or) inclusions precluded accurate optical determination of feldspar composition in many sections. In some fine-grained rocks the feldspar was determined by relative refractive index only. When the refractive index of the feldspar was less than that of Canada balsam, orthoclase could not be distinguished from albite, and such feldspar was called "alkali feldspar." Microcline grid twinning was observed in some low-refractive-index feldspars.

Plagioclase in the quartzofeldspathic rocks comprises three broad compositional groups:

1. Cloudy untwinned low-refractive-index feldspar—probably albite—intimately associated with epidote and (or) calcite as pseudomorphs of plagioclase in tuffs and flows.
2. Cloudy twinned relict phenocrysts in tuffs and flows, having an anorthite content of 17–38 percent.

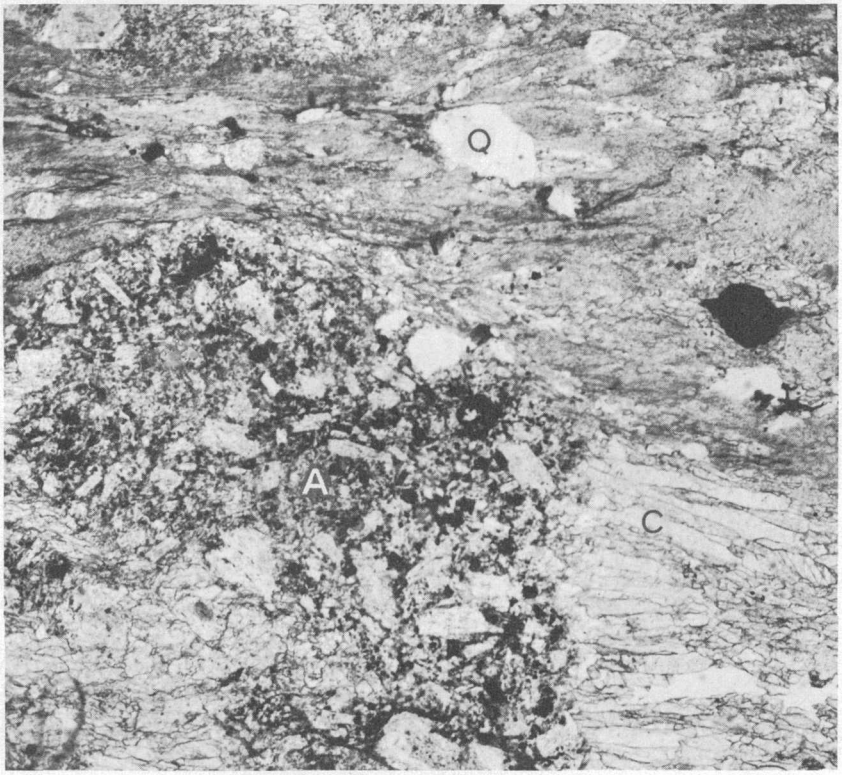

FIGURE 22.—Crystalline lithic tuff. Andesite fragment has rods of calcite in its "shadow." C, calcite; A, andesite fragment; Q, quartz. Long dimensions of calcite rods parallel foliation in rock section. Section matrix is composed mostly of biotite and chlorite. × 40. Koip sequence.

FIGURE 23.—Crystalline lithic wacke. Angular fragments of quartz, feldspar, and volcanic rocks in a recrystallized matrix of biotite, muscovite, and quartz. Major foliation (parallel to long dimension of figure) is intersected and crinkled by a second foliation. × 40. Koip sequence.

3. Minute granules of high-refractive-index feldspar that are sometimes twinned. An anorthite content of 45±5 percent could be determined on only one grain of this plagioclase because of the small grain sizes. Relative refractive indices indicate that some of this plagioclase is even more calcic than An_{45}.

Plagioclase in the basic mineral assemblages comprises two compositional groups:

1. Plagioclase having an average anorthite content of 8 percent. The extreme anorthite percentages in this group are 3 and 13 percent.
2. Plagioclase having an average anorthite content of 25 percent. The extreme anorthite percentages in this group are 23 and 29 percent.

Mica.—White mica and biotite generally show at least one preferred orientation. Biotite occurs as ragged subhedral crystals that are pleochroic in shades of brown and green. White mica, $2V_x=40°$,

occurs as subhedral crystals. Chlorite (pale green to colorless; $2V_z$, small; anomalous birefringence in shades of brown and "berlin blue") is present as an accessory phase in many sections.

Amphibole.—Amphibole in quartzofeldspathic rocks is probably tremolite (pleochroic, from light green to colorless; $2V_x$, large) and in basic assemblages is either actinolite or hornblende ($2V_x$, large; pleochroic, from light green to yellow green). A colorless amphibole in a hornfels in the Log Cabin Mine pendant is cummingtonite ($2V_z$, large; birefringence, to second-order orange).

Epidote.—Epidote minerals commonly occur as pseudomorphs after plagioclase, as a vein mineral associated with quartz, and as disseminated anhedral crystals. Pistacite, clinozoisite, and zoisite were all identified. Viewed in parallel light, some varieties of pistacite are pale yellow green or brown and pleochroic, and other varieties are colorless; birefringence may be anomalous, in shades of blue and yellow. Clinozoisite is colorless and has anomalous birefringence;

FIGURE 24.—Muscovite-biotite schist. Bedding-plane foliation is crinkled by a second cleavage. × 40. Koip sequence.

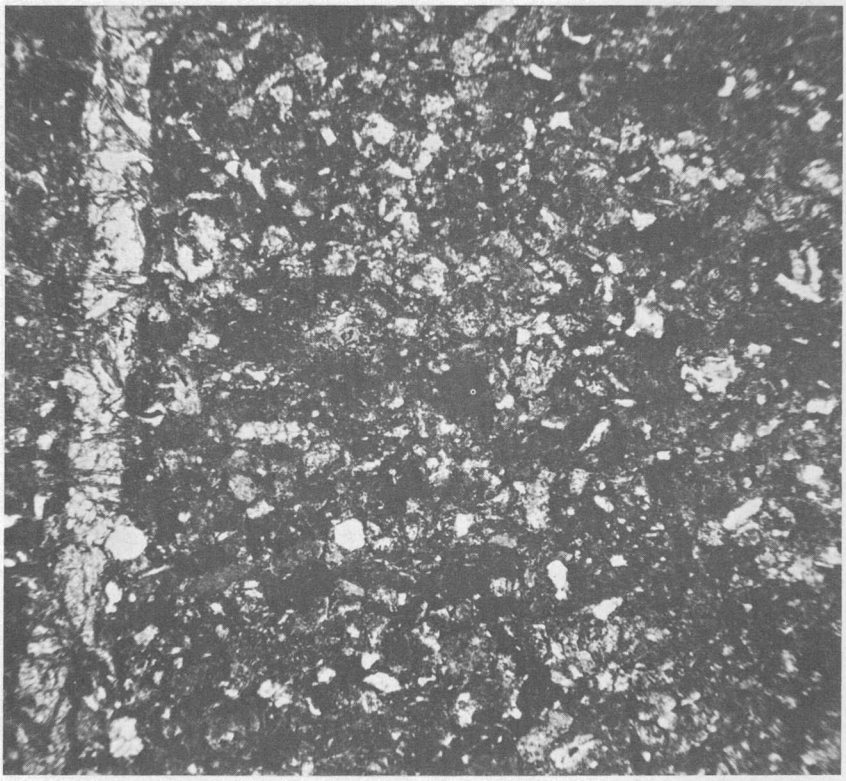

FIGURE 25.—Subfeldspathic lithic wacke. Coarse-vein mineral is epidote. × 40. Dana sequence.

$2V_z$ is large, and dispersion may be extreme. Zoisite occurs as large anhedral crystals having low birefringence; $2V_z$ is about 30°.

Clinopyroxene.—Pyroxene—in the diopside-hedenbergite series—is colorless or pale green in parallel light and is optically positive. It occurs as granular aggregates or as large anhedral crystals.

Wollastonite.—Wollastonite ($2V_x$, small, Y=b; low birefringence) occurs as large plates that may be twinned. In some skarns, wollastonite is poikiloblastic to granular diopside.

Calcite.—Calcite occurs associated with albite in pseudomorphs of plagioclase, as a vein mineral associated with quartz, and as disseminated anhedral crystals.

Andalusite.—Andalusite occurs as euhedral crystals of the variety chiastolite or as colorless anhedral crystals.

Garnet.—In skarns and calc-silicate hornfels, garnet occurs as colorless to yellow-brown grossularite-andradite. In schists it occurs as colorless to red-brown almandine.

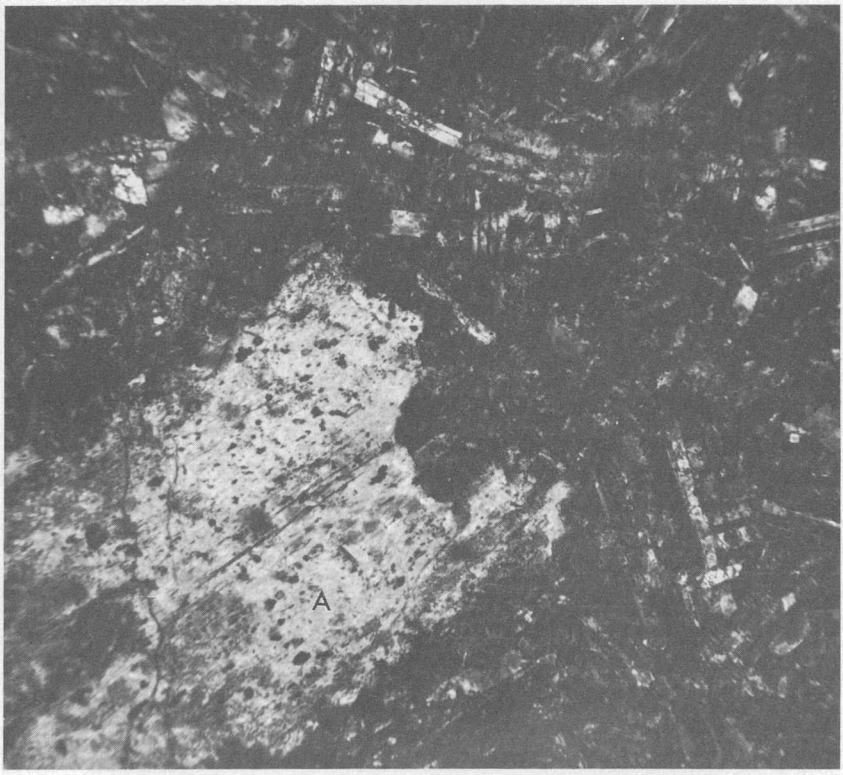

FIGURE 26.—Metamorphosed basalt. Amphibole (A) pseudomorphs pyroxene. Plagioclase is acid labradorite. × 40. Dana sequence.

DEFORMATION

GENERATIONS OF FOLDING

The structural complexity of the metamorphic rocks increases with geologic age. Three distinct deformations have been identified from study of the geometrical relations between folds of different styles and orientations. (See Weiss, 1959a, for a discussion of the geometry of superposed folds). Folds of one style deformed by folds of another style and the presence or absence of a specific generation of folds in a rock sequence were the principal criteria used to establish the folding history. The study showed a different average orientation of axial surface for each of the three generations of folds, as follows:

1. First-generation folds.—These folds occur only in the Lewis sequence. They are best exposed in the Log Cabin Mine roof pendant, where deformation subsequent to their formation has been minor and they have retained their original orientation and geometry. They have appressed limbs, simple hinges (fig. 5), and

axial planes that strike about north and are vertical or dip moderately to the west.

2. Second-generation folds.—These occur in both the Lewis and the Koip sequences. They have appressed limbs, simple hinges that may be disrupted by axial-plane cleavage (figs. 6, 12), and vertical axial surfaces that strike northwest.
3. Third-generation folds.—These folds occur in all the rock sequences. They are open, have simple hinges, and have steep axial surfaces (fig. 13) that strike N. 50°–70° W.

Collective diagrams of poles to attitudes of beds and of axial planes, and collective diagrams of fold axes and lineations measured were plotted in lower hemisphere projection on an equal-area net for each of the four major roof pendants studied; separate diagrams are shown of these structural elements for each rock sequence in the Ritter Range pendant (pl. 1). In each pendant and in each sequence, a β axis was determined. This axis is the normal to the girdle of poles to bedding attitudes and is the indirectly determined (statistically significant) fold axis for the area designated. Diagrams will be considered first in the youngest, least deformed rocks, and last in the oldest, most deformed rocks.

In the Dana sequence, only third-generation folds were observed. A diagram of poles to attitudes of beds measured in this sequence is shown on plate 1, 1*A*. This girdle defines a horizontal β axis that trends about N. 48° W. Subvertical cleavages are parallel to axial surfaces of the few minor folds observed and strike about N. 50° W.

Both second- and third-generation folds were observed in the Koip sequence. Diagrams of poles to attitudes of bedding and axial planes and of fold axes are shown on plate 1 (*2A*, *2C*, *2B*, respectively). A single β axis in bedding is not defined in these Permian(?) rocks. Instead, there are two indirectly determined fold axes that are coincident with the two maximums of plots of lineations and small-fold axes. These fold axes lie in a vertical plane that strikes about N. 50° W. Axial plans in the Koip sequence strike northwest and are steeply dipping or vertical.

The collective diagrams of bedding attitudes and fold axes in the Koip sequence (pl. 1, 2*A* and 2*B*) can be divided into three domains, each defined by a single axis of cylindrical folding (fig. 27). Attitudes of bedding in domain 1 define a fold axis that plunges 43° N. 47° W. (fig. 27*A*), and in domain 2, a fold axis that plunges 70° S. 50° E. (fig. 27*B*). Domain 3, on Mount Dana and Mount Gibbs, is folded ito a syncline whose axis trends identically with that in domain 1. The lineations and small-fold axes measured in each domain, when plotted

on an equal-area net, have a contour maximum that coincides with the β axis for that area.

Axial surfaces of most minor folds measured in the Koip sequence are parallel to the axial surfaces of the third-generation folds in the Dana sequence. This suggests that the minor folds measured in the Koip sequence are mostly third-generation folds, and the two maxi-

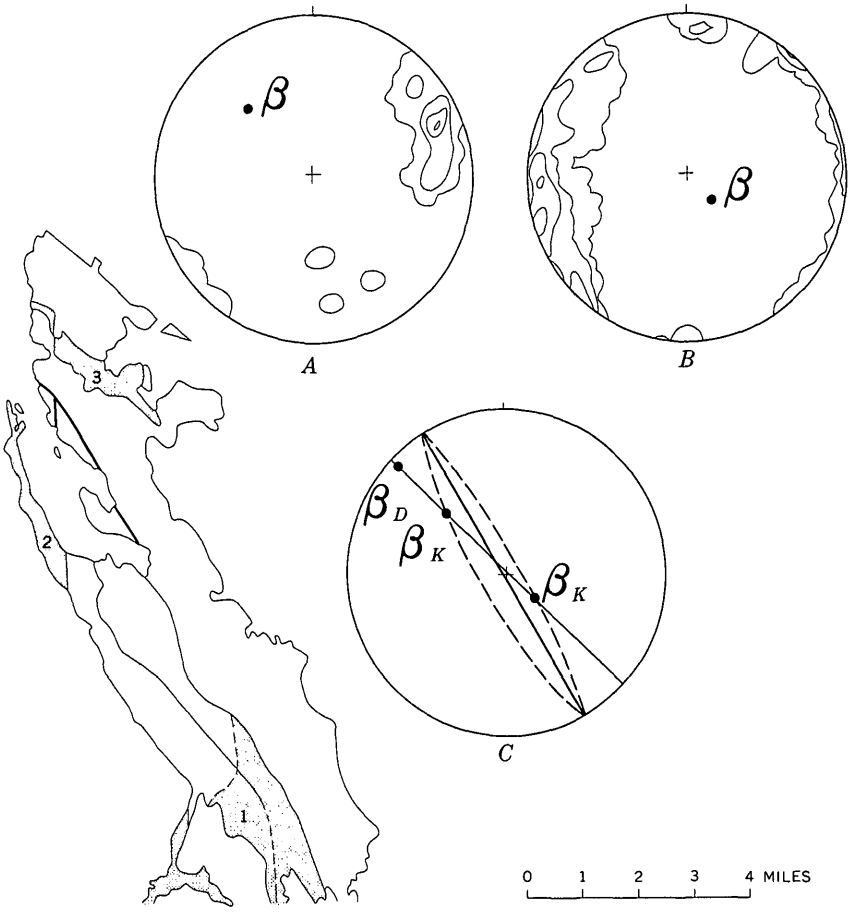

FIGURE 27.—Structural geometry of domains (stippled areas) in the Koip sequence and synoptic geometry of β axes and axial planes in the Koip and Dana sequences. *A*, Diagram of poles to attitudes of 42 beds in domain 1. Contours are 2.3, 10, 20 and 30 percent of 1-percent area. *B*, Diagram of poles to attitudes of 70 beds in domain 2. Contours are 1.4, 4, 6, and 10 percent of 1-percent area. *C*, Synoptic diagram of third-generation fold axes and principal axial surfaces in the Koip and Dana sequences. β_K and β_D are the third-generation fold axes in the Koip and Dana sequences, respectively. Solid lines represent axial planes; dashed lines represent dominant bedding attitudes in the Koip sequence after second-generation folding.

mums in the collective diagram of fold axes represent plunging third-generation folds.

Plunging folds and lineations can form in three main ways (Weiss, 1959b, p. 34), as follows:

1. A single triaxial strain can produce fold axes plunging at any angle in initially horizontal slip surfaces. The plunge of the fold axes can change with progressive deformation; in general, it steepens.
2. Oblique squeezing of previously folded slip surfaces produces fold axes on the limbs of the folds. These axes plunge at angles controlled by the direction of squeezing and the attitudes of the limbs. (See also McBirney and Best, 1961.)
3. A fold axis may be tilted by later folding.

A synoptic diagram of third-generation fold axes and principal axial surfaces in the Koip and Dana sequences is shown in figure 27*C*. This distribution of fold axes is best explained as having resulted from an orogeny (simple compression) that affected subhorizontal rocks of the Dana sequence lying unconformably over previously deformed rocks of the Koip sequence. The previous deformation of the Koip sequence produced isoclinal second-generation folds that had vertical axial surfaces. The third-generation fold axes in the Koip sequence are the lines of intersection between the limbs of second-generation folds and the third-generation axial surface; in the Dana sequence, the line of intersection between subhorizontal bedding and the third-generation axial surface. The inferred dominant bedding attitudes in the Koip sequence after second-generation folding are compatible with the observed isoclinal minor second-generation folds (fig. 12).

First-, second-, and third-generation folds were observed in the Lewis sequence. Diagrams of poles to attitudes of beds and axial planes and of fold axes measured in these Paleozoic rocks are different in each of the four major roof pendants studied. In the Ritter Range pendant the girdle of poles to attitudes of beds defines a β axis that plunges 55° N. 30° W., this girdle is also coincident to the contour maximum of minor fold axes for the same area (pl. 1, 3*A* and 3*B*). Although this fold axis is the most significant structural trend in the pendant, the spread of structural elements and the definition of the two axial-plane maximums in the diagram suggest that more than one cylindrical β axis is present. In the Saddlebag Lake roof pendant, the attitudes of poles to beds and of minor fold axes define a β axis that plunges 25° N. 30° W. (pl. 1, 4*A*, 4*B*). The diagrams show that a β axis that plunges 70° S. 30° E. is the principal axis in the Gull Lake roof pendant (pl. 1, 5*A* and 5*B*). Dispersion of points repre-

senting all structural elements shows, however, that folding is very complex in this pendant; the steeply dipping axial planes range in strike from north to N. 60° W. A β axis that plunges 25° S. 5° W. and an axial surface that strikes north and dips about 45° W. are represented in the diagrams for the Log Cabin Mine roof pendant (pl. 1, 6*A* and 6*B*). In this pendant, however, the bedding poles permit, and the fold axes indicate, considerable dispersion of this axis within the axial plane.

First-generation folds were only slightly modified by subsequent deformation in the Log Cabin Mine roof pendant but were greatly deformed by later folding in the Gull Lake roof pendant. The younger folds, and those in the Lewis sequence in the Ritter Range and Saddlebag Lake pendants, are considered to be second- and third-generation folds because their axial surfaces (pl. 1, 3*C* and 5*C*) strike in the same direction as the axial surfaces of second- and third-generation folds in the Koip and Dana sequences. Because of their similar styles and orientations, second- and third-generation folds in the Lewis sequence are difficult (or impossible) to distinguish unless they occur in the same outcrop.

A synoptic diagram of the principal fold axis in bedding in the Lewis sequence for each of the four major roof pendants studied is shown in figure 28. The statistical fold axes of the Ritter Range, Gull Lake, and Saddlebag Lake roof pendants lie in a plane coincident with the axial plane of second-generation folds and are therefore interpreted to be primarily the result of second-generation folding. The plunging second-generation fold axes determined for the Lewis sequence are interpreted to be the result of superposed folding of rocks already deformed by first-generation folds. The second-generation fold axis in each roof pendant is the line of intersection between the second-generation axial surface and the dominant bedding surface in that area caused by first-generation folding. First-generation folds in the Lewis sequence in all but the Gull Lake pendant had axial surfaces with an initial strike of north and dip of about 45° W. After the first-generation folding occurred, most bedding in these pendants dipped moderately to the west. Also, after first-generation folding most beds in the Gull Lake pendant had a north strike and a steep dip to the east. The dispersion of points around the point maximums in the diagrams for the Lewis sequence is due to third-generation folds.

The relatively small effect of the third deformation on the structural geometry of the Lewis sequence indicates that the second deformation was the more severe in this part of the Sierra Nevada. The isoclinal second-generation folds in the Koip sequence, as opposed to the third-generation folds in both the Koip and Dana sequences, support the observation that the second deformation was the more severe.

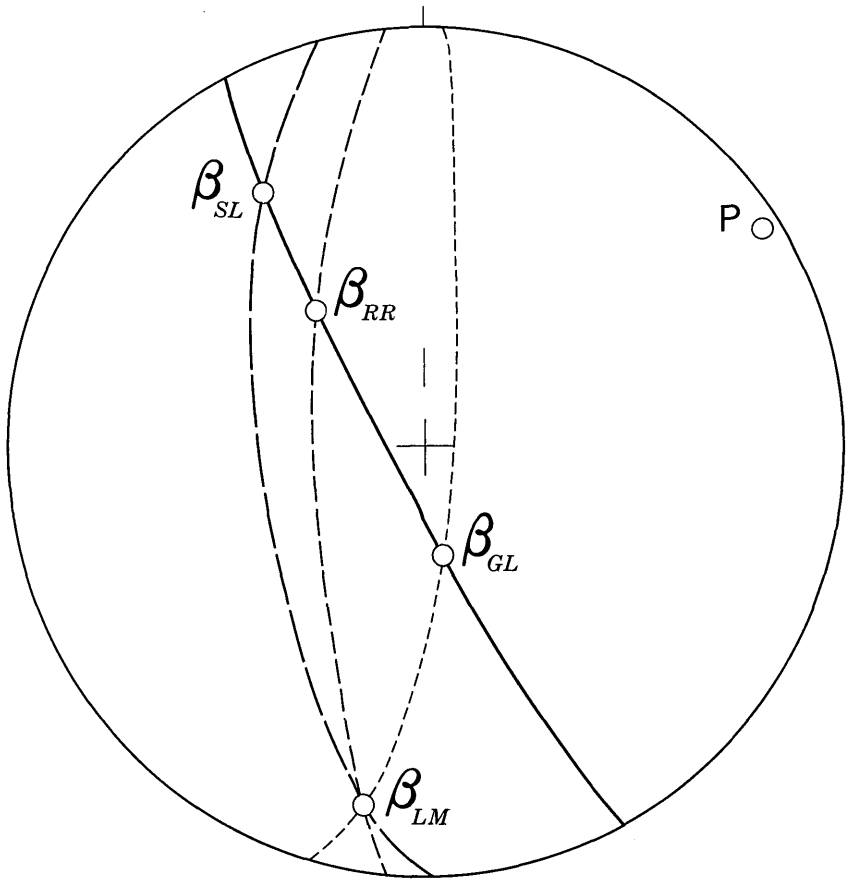

FIGURE 28.—Synoptic diagram of principal fold axes in the Lewis sequence. Axes for the Gull Lake, Ritter Range, Saddlebag Lake, and Log Cabin Mine roof pendants are, respectively, β_{GL}, β_{RR}, β_{SL}, and β_{LM}. The solid line is the axial surface of the second deformation with pole designated "P." Dashed lines represent attitudes of bedding about first-generation folds determined by the great circles passing through β_{LM} and the second-generation fold axis in each roof pendant.

EXTENT AND CAUSE OF DEFORMATION IN THE PENDANT ROCKS

Determination of the causes of deformation in the intruded roof rocks and wallrocks is critical to the study of several problems related to the origin of the composite Sierra Nevada batholith. Two general cases are considered.

1. Structures in the roof pendants were caused by the forceful emplacement of bordering plutons and are limited to individual pendants.

2. Emplacement of plutons was passive, and structures in the pendants were caused by regional forces and can be traced from pendant to pendant.

If some deformations are regional, the problem of their temporal correspondence to plutonism can be investigated.

In complexity folded rocks, structural geometry alone does not distinguish a single complex deformation from two or three separate simple deformations. The folds observed in the roof pendants of the Mono Craters quadrangle evidently are primarily the result of three successive major regional deformations. Evidence of a fourth deformation is present locally.

Of the three generations of folds recognized in the metamorphic rocks of the quadrangle, three affected the oldest, Lewis sequence; two affected the middle, Koip sequence; and one affected the youngest, Dana sequence. The observed structural orientations in these metamorphic rocks are those that could be predicted by the geometry of superposed folding. That structural complexity of a rock sequence is a function of its age and not of proximity to plutons indicates that a mechanism other than forceful emplacement of granitic magma caused the folding in the metamorphic rocks, and that several separate deformational episodes affected the area.

Parker (1961) summarized the available data concerning fold axes and lineations in metamorphic rocks for a large part of the Sierra Nevada. He observed that the wide variation in orientation of these features showed that a complex geometry exists in the metamorphic rocks and that steep lineations and fold axes predominate. The widespread presence of steep fold axes suggests that the majority of exposed metamorphic rocks of the Sierra Nevada have been subjected either to more than one deformation or to a single complex deformation.

Ramsay (1958) stated that axial surfaces are the most regular feature of contemporaneously formed folds. Kistler and Bateman (1966) showed the initial orientation of axial surfaces which they interpreted for first-generation folds in the Dinkey Creek roof pendant in the central Sierra Nevada to be the same as those observed in first-generation-fold axial surfaces in the Log Cabin Mine roof pendant (55 miles to the north), as discussed in this report. Strikes of axial surfaces of folds in those roof pendants and in Sierra Nevada wallrocks that have been studied in detail are shown in figure 29. The number of axial surfaces, the orientations of axial surfaces, and the age of the strata, where known, are summarized in table 4.

TABLE 4.—*Number of deformations determined in several roof pendants and areas of wallrock in the Sierra Nevada*

[Letters in boxheads refer to areas designated in figure 29. Bracketed numbers indicate number of deformations determined in each area. Strikes of axial surface at each locality are also shown. Oldest folds are at bottom]

A Clark and others (1962)	*B* Parker (1961)	*C* Baird (1962)	*D* Clark and others (1963)	*E* Best (1963)	*F* Kistler (this report)	*G* Kistler and Bateman (1966)	*H* Kistler and Bateman (1966)	*I* Christensen (1963)	*J* Rinehart and Ross (1964)	*K* Bateman (1965)
Lower Jurassic			Jurassic [1] N. 30° W.	Upper Jurassic [2] N. 25° W. N. 40° W.	Lower Jurassic [1] N. 50° W.			Upper Triassic [1] N. 25° W.		
Upper Triassic (?) [1] N. 30° W.	Triassic(?) [1] N. 35° W.									
Angular unconformity			?	?	Angular unconformity					
					Permian [2] N. 50° W. N. 30° W.		Permian and Triassic(?) [2] N. 60° W. N. 25° W.			
					Angular unconformity					
Silurian (?) [>1]		Paleozoic [3] N. 25° W. N. 60° E. NW.			Pennsylvanian(?) and Permian(?) Ordovician(?) and Silurian(?) [3] N. 50° W. N. 30° W. N.	Paleozoic(?) [3] N. 60° W. N. 25° W. N. 5° E.			Ordovician and Silurian(?) [1] N.	Ordovician and Silurian(?) [1]. N.

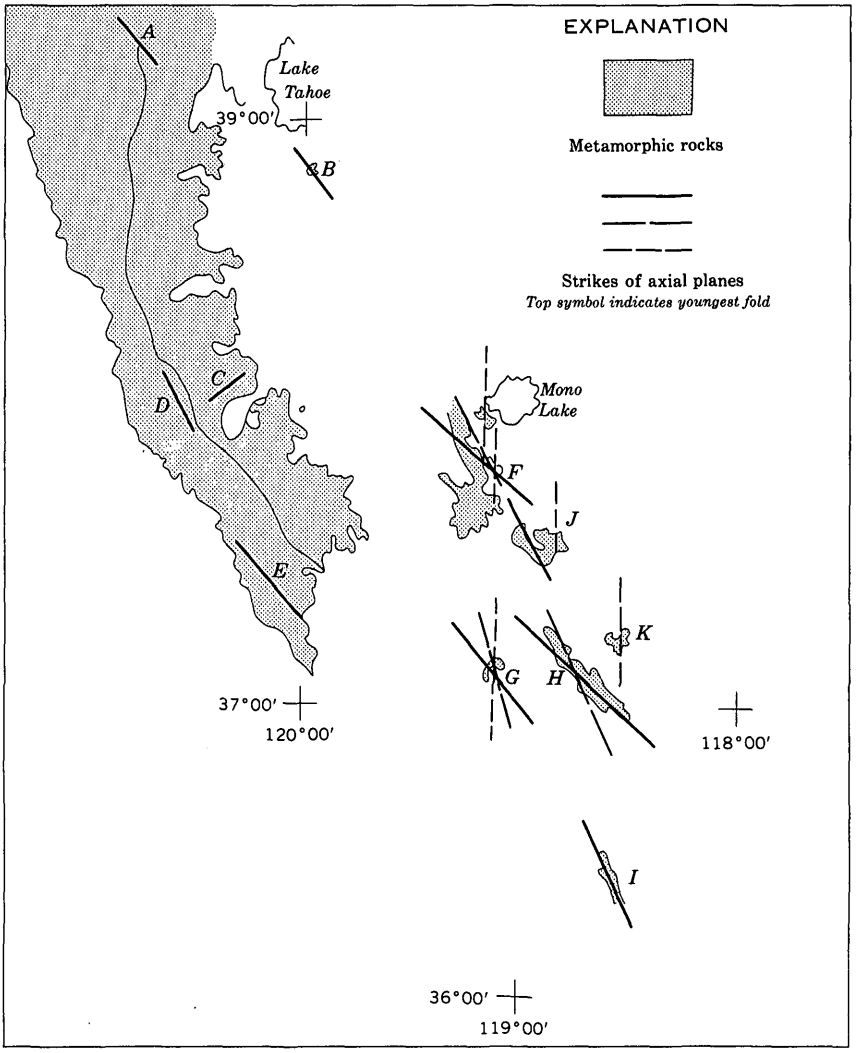

FIGURE 29.—Strike of axial surfaces of folds in deformed wallrocks and roof rocks in the Sierra Nevada. Reference to lettered localities is given in table 4. Trends of planes that are thought to be contemporaneous have the same symbol.

The record of a single major deformation is evident in Upper Triassic and younger strata in the Sierra Nevada. Folds formed in this deformation are characterized by steep to vertical axial surfaces that generally strike about N. 50° W. between lats 37° N. and 38° N., and about N. 25° W. at lats 36° N. and 39° N. (See fig. 29.) Upper Jurassic rocks in the vicinity of Mariposa (Best, 1963) were affected by a later deformation that produced folds locally.

In the Permian and older rocks, the effects of one or two deformations are evident in addition to the folds formed in the deformation recorded in the Upper Triassic and younger metamorphic rocks.

Of the additional deformations, the younger is considered to have been the first to affect the Permian(?) volcanic rocks of the Koip sequence, and the second to have folded the Paleozoic rocks of the Lewis sequence. These folds are recognized as the second deformation in the Dinkey Creek roof pendant and as the first deformation in the Goddard pendant (Kistler and Bateman, 1966). The resultant folds have steep to vertical axial surfaces that strike from N. 20° W. to N. 30° W. between lats 37° N. and 38° N.

The earlier of these additional deformations was apparently the first deformation in the Lewis sequence in the Mono Craters quadrangle and in the metamorphosed sedimentary rocks of the Dinkey Creek pendant (Kistler and Bateman, 1966). Folds produced by the deformation are generally overturned eastward and have axial surfaces that strike north and dip from 45° W. to vertically. Other folds in this system have been recognized in the lower Paleozoic rocks of the Mount Morrison pendant (Rinehart and Ross, 1964) and in the Bishop Creek pendant (Bateman, 1965).

Temporally related folds that have uniform axial-surface attitudes for long distances strongly support the author's conclusion that several distinct regional deformations have affected the metamorphosed pendant and wallrocks of the Sierra Nevada.

AGES OF THE DEFORMATIONAL EPISODES

The three deformations recognized in the metamorphic rocks in the Mono Craters quadrangle occurred on a regional scale in the Sierra Nevada. The age of each deformation is bracketed by the ages of the youngest rocks folded and the oldest rocks not folded during that deformation. Ages of the deformations that resulted in first- and second-generation folds are most closely bracketed by the ages of the rock sequences in the Mono Craters quadrangle; the age of the deformation that caused third-generation folds is bracketed most closely by the ages of rock units in the foothill belt of the Sierra Nevada.

The first deformation to effect the metamorphic rocks in the Mono Craters quadrangle resulted in first-generation folds and is considered equivalent to the Sonoma orogeny described by Silberling and Roberts (1962, p. 36) in western Nevada. First-generation folds were observed in Pennsylvanian(?) and Permian(?) sedimentary rocks of the Lewis sequence but not in Permian(?) sedimentary and volcanic rocks of the Koip sequence. The Sonoma orogeny is dated as Permian in the China Mountain area of the Golconda quadrangle, where rocks of Pennsylvanian and Permian age are tightly folded and thrust

faulted and overlain unconformably by the Koipato Formation (Permian and Early Triassic).

The deformation that caused second-generation folds in the Mono Craters quadrangle occurred in the Early or Middle Triassic. This is indicated by the facts that this fold system deforms the Permian(?) Koip sequence but not the Lower Jurassic Dana sequence, and that it is not recognized in either the Upper Triassic rocks of the Mineral King roof pendant (Christensen, 1963) or in the Triassic(?) rocks of the pendants near Ebbetts Pass (Parker, 1961).

Third-generation folds in the quadrangle were probably formed during the Late Jurassic Nevadan orogeny; they occur in all metamorphic rocks in the quadrangle and are a result of the only deformation recognized in the Lower Jurassic Dana sequence. In the Upper Jurassic Mariposa Formation of the western foothill belt of the Sierra Nevada, folds thought to be equivalent to third-generation folds are truncated ern foothill belt of the Sierra Nevada (Curtis and others, 1958).

TEMPORAL RELATION OF DEFORMATIONAL EPISODES TO GRANITIC INTRUSIONS

Three periods of granite emplacement in the Mesozoic have been determined in the Sierra Nevada (Kistler and others, 1965). Dated granitic rocks in the Mono Craters quadrangle fall into two age groups (fig. 30). The quartz monzonite of Lee Vining Canyon (190 m.y.) and the granodiorite of Mono Dome (206 m.y.) are Late Triassic and Middle Triassic by Kulp's time scale (1961). They crop out east of the Ritter Range pendant and were emplaced during the older of the two periods of magma emplacement recognized in the east-central Sierra Nevada (Kistler and others, 1965). The granodiorite of Kuna Crest, which crops out west of the Ritter Range pendant, belongs to the youngest (Late Cretaceous) period of magma emplacement recognized in the Sierra Nevada (Evernden and others, 1957; Kistler and others, 1965; Hurley and others, 1965). Biotite in the older plutons, in the eastern part of the quadrangle, is young, owing to the high thermal gradient produced during emplacement of the younger Cretaceous plutons to the west. A third period of magma emplacement, intermediate in age between the two periods of the eastern Sierra Nevada, is defined by the potassium-argon ages of biotite from granitic rocks in the western foothill belt of the Sierra Nevada (Curtis and others, 1958).

Two Mesozoic deformations of regional extent are recognized in the metamorphic rocks of the Sierra Nevada. The earlier of these deformations occurred in the interval between Late Permian(?) and Late Triassic; the Late Triassic–Early Jurassic period of plutonic emplacement is possibly related to this event. The second deformation was the Late Jurassic Nevadan orogeny; the Late Jurassic period

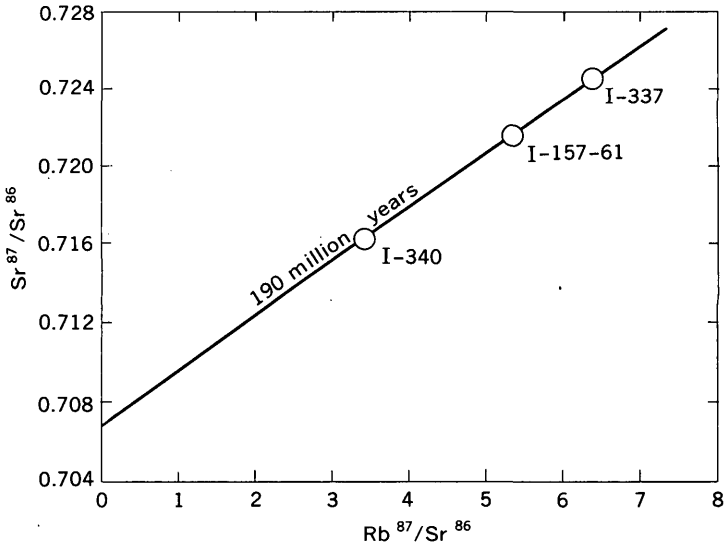

Sample	Rb (ppm)	Sr† (ppm)	Sr^{87}/Sr^{86} *	Rb^{87}/Sr^{86}
I-340	160	140	0.7160	3.34
I-157	156	85.8	.7211	5.30
I-337	185	86.3	.7243	6.26

* Unspiked—normalized to an 86/88 ratio of 0.1194.
† Normal strontium.

Granodiorite	Potassium (K) (weight percent)	Argon (Ar) (moles per g $\times 10^{-11}$)	Radiogenic argon (percent)	Age (millions of years)
Kuna Crest	6.82	102.2	84	82.6
Mono Dome:				
Biotite	6.25	93.9	68	82.3
Hornblende	.446	20.6	72	206

FIGURE 30.—Rubidium-strontium whole-rock age determinations for quartz monzonite of Lee Vining Canyon (1st table above), and potassium-argon age determinations of biotite or hornblende for granodiorite of Kuna Crest and granodiorite of Mono Dome (2d table above). Explanation (1st table): Ratio radioactive rubidium (Rb^{87}) to total rubidium, 0.283 g Rb^{87} per g Rb; rubidium decay constant, $\lambda_\beta = 1.47 \times 10^{-11}$ year^{-1}. Explanation (2d table): Potassium decay constants, $\lambda_\epsilon = 0.584 \times 10^{-10}$ year^{-1}, and $\lambda_\beta = 4.72 \times 10^{-10}$ year^{-1}; radioactive potassium (K^{40}) to total potassium, 1.22×10^{-4} g K^{40} per g K.

of magma emplacement (Curtis and others, 1958) may have been the last phase of this event.

No regional deformation correlative with the Cretaceous period of magma emplacement has been recognized in the Sierra Nevada. The deformation and recrystallization that the metamorphic rocks had undergone before Late Cretaceous time however, probably made them insusceptible to further deformation. Nevertheless, a second deformation of the Upper Jurassic Mariposa Formation has been recognized locally in the western foothills (Best, 1963), and a Cretaceous deformation has been recognized east of the Sierra Nevada in the Jackson Mountains of western Nevada (Willden, 1958). One or both deformations may be related to the Cretaceous plutonism in the Sierra Nevada.

No intrusive rocks related to the earliest deformation, which is probably correlative with the Sonoma orogeny, have been recognized in the Sierra Nevada or immediate vicinity. Volcanism immediately followed this deformation, however, and the character of sedimentation changed radically in the Mono Craters region of the Sierra Nevada; older plutons may yet be found.

CONDITIONS OF METAMORPHISM

Multiphase deformation and plutonic activity have complexly metamorphosed the rocks in the quadrangle; the older granitic rocks have been subjected to both regional and thermal metamorphism. Despite the complexities such as schists, hornfelses, and skarns occurring close together, some general observations can be made about the products of the metamorphism.

Skarns occur close to or in contact with granitic plutons. Hornfels and schists occur either in contact with granitic plutons or in the interior of pendants. Contact metamorphism produced rocks of the hornblende hornfels facies; but the process was not simple for the plutons that caused it were intruded at widely separated intervals.

Regional metamorphism of Barrovian type produced mineral assemblages in the almandine amphibolite facies. The physical conditions that cause the formation of the minerals of this facies were temperatures of about 400°–700°C and pressure equivalent to that at a depth of about 10 km (Fyfe and others, 1958, p. 218, 228). These conditions possibly occurred in the rocks of the Lewis and Koip sequences in the Ritter Range and Gull Lake pendants. However, rocks of the Lower Jurassic Dana sequence were probably never buried to a depth of 10 km, because they do not have textures generally associated with the amphibolite facies of metamorphism. High fluid pressures, transitional to those of regional metamorphism, possibly

existed in the Dana sequence during the intrusion of the Cretaceous granitic rocks into the Ritter Range pendant. If so, these pressures would have permitted epidote and scapolite to be stable in the presence of calcic plagioclase. Best (1963, p. 119) proposed that a similar mechanism explains the "anomalous" occurrence of epidote in rocks metamorphosed to the hornblende hornfels facies in aureoles surrounding granitic intrusions in the western foothills of the Sierra Nevada.

FAULTING

RANGE-FRONT FAULTS

Russell (1889) was the first geologist in the region to recognize that the east front of the Sierra Nevada is a fault scarp. Two zones of Sierra Nevada frontal faults cut diagonally across the Mono Craters quadrangle (fig. 31). The west zone is continuous across the area, but the east zone is divided by an embayment.

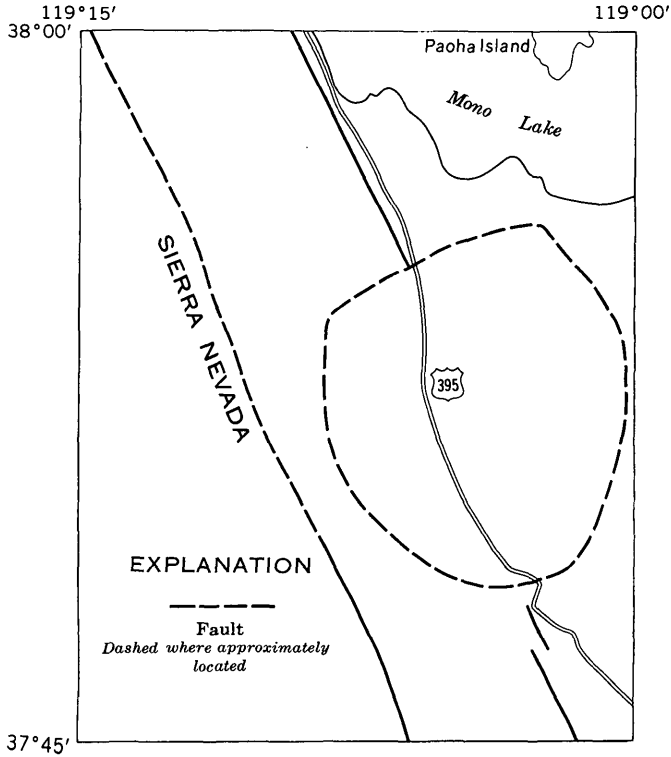

FIGURE 31.—Range-front faults bordering the Sierra Nevada in the Mono Craters quadrangle.

The west fault zone can be traced for 18 miles across the quadrangle on the basis of the following criteria:

1. Thin mylonite lenses in a granodiorite in the northwestern part of the quadrangle.
2. Abrupt change in the range-front slope east of Dana Plateau, Mount Gibbs, Mount Lewis, and Mount Wood.
3. Juxtaposition of xenolith-laden quartz monzonite to xenolith-free quartz monzonite east of Dana Plateau and Mount Gibbs.
4. Offset of Sherwin Till east of Mount Gibbs, Mount Lewis, and Mount Wood.
5. Slotlike valley etched out by ice along the fault trace south of Silver Lake. (See Putnam, 1949, pl. 6, fig. 2.)

If the isolated remnants of till near the crest of the Sierra Nevada in the quadrangle are of Sherwin age, about 1,000 feet of vertical displacement occurred in the west fault zone after Sherwin Glaciation and before Tahoe Glaciation.

The east fault zone can also be traced across the quadrangle, except between June Lake and Williams Butte. In the northern part of the quadrangle the fault trace is along the base of the bedrock scarp that rises abruptly from Mono Lake, and it roughly parallels the west boundary of the Mono Basin subsidence, as determined geophysically by Pakiser and others (1960). South of Williams Butte the scarp terminates abruptly, but east of June Lake it begins again and can be traced past the south edge of the quadrangle. The latter trace is irregular in trend and can be recognized by vertical displacement of about 300 feet of the Bishop Tuff. Relative movement is west side upward in both fault zones.

The dips of the range-front faults were not measured, but the fault traces on the map (particularly those of the west zone) indicate that the dips are very steep, if not vertical. Most of the displacement along both zones occurred after Sherwin Glaciation and before Tahoe Glaciation. The east zone, however, was probably active more recently than the west zone because it displaces the Bishop Tuff.

RANGE-FRONT EMBAYMENT

A major shear zone that has features of the gneissic and mylonitic facies of the Colville batholith (Waters and Krauskopf, 1941) extends with a curved trace from the south end of Grant Lake for about 5 miles northwestward (fig. 32). The shear zone borders a pluton of hornblende-bearing quartz monzonite that crops out discontinuously in the east-central part of the quadrangle and is believed to be protoclastic. The trace of the zone is not continuous; it is covered in places by moraines of Tahoe and Tioga ages or by the waters of Grant Lake.

At Grant Lake the shear zone, composed of mylonite (fig. 33) and crushed quartz monzonite, marks the contact between hornblende-bearing quartz monzonite and porphyritic quartz monzonite. Above the Tioga lateral moraine northwest of Grant Lake, the mylonite outcrop is about 100 feet wide. Large augen of hornblende-bearing quartz monzonite are enclosed in a black flinty matrix. Small outcrops of highly fractured quartz monzonite also occur here and mark the zone to the northwest, where a large outcrop of the sheared quartz monzonite protrudes through the Tioga moraine. The rock is broken into hand-specimen-size pieces that are bounded by fractures of many attitudes. Fracture surfaces are slickensided, and the striations range in plunge from horizontal to vertical. The northernmost exposure of

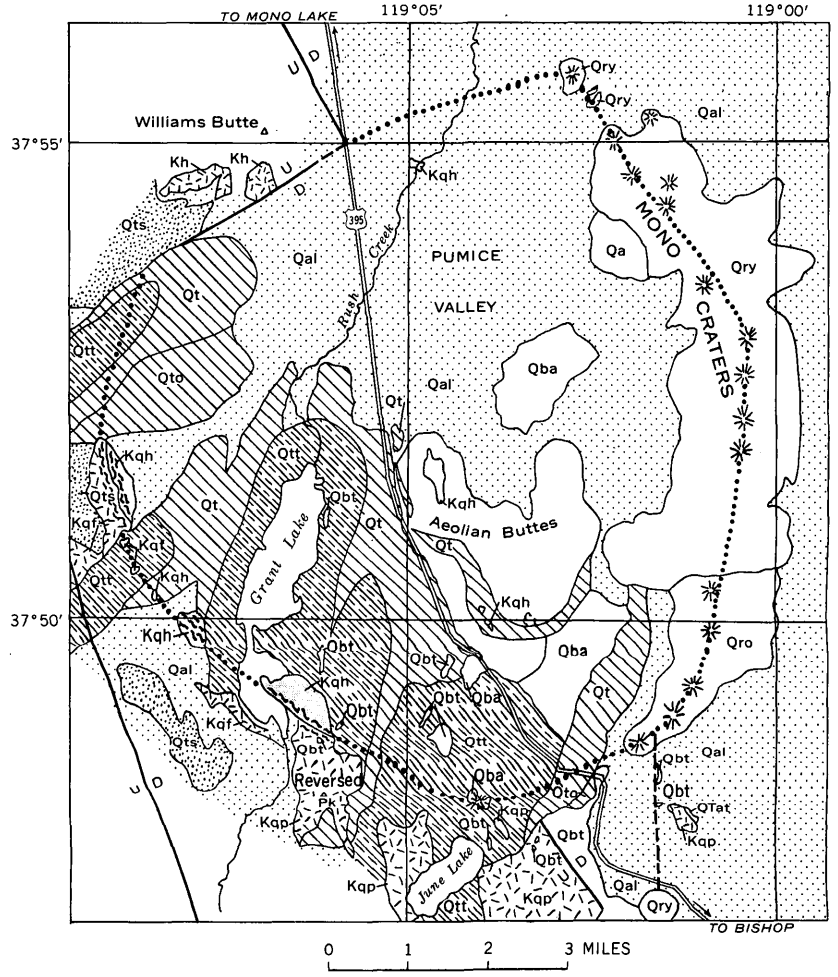

FIGURE 32.— Geology of the Mono Craters vicinity.

EXPLANATION

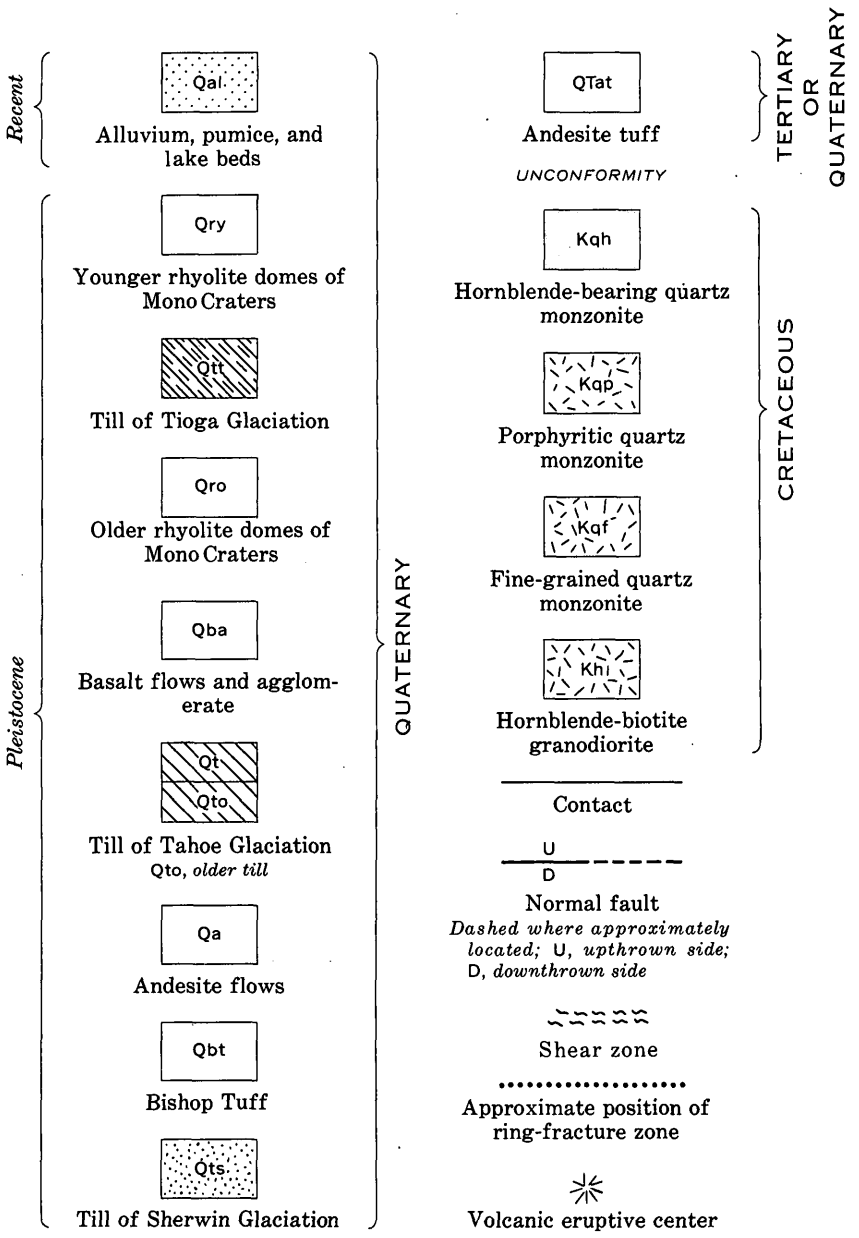

FIGURE 32 (Explanation).

FIGURE 33.—Mylonite near contact between hornblende-bearing quartz monzonite and porphyritic quartz monzonite at Grant Lake. Sheared rock in photograph is hornblende-bearing quartz monzonite. Aplite dike intrudes mylonite.

the shear zone is a low hill composed entirely of intensely fractured quartz monzonite and thin bands of mylonite. Here, too, the fractures have diverse attitudes, and slickensides plunge at any angle. The shear zone here marks the contact between the hornblende-bearing quartz monzonite and fine-grained quartz monzonite.

Locally the mylonite is recrystallized to form blastomylonite and mylonitic gneiss (Waters and Krauskopf, 1941, p. 1408). As in the Colville batholith, the recrystallized mylonite is intimately associated with, and grades into, mylonite and is best explained as a product of autometamorphism. The close similarity of these shear-zone features to features of the protoclastic zone at the Colville batholith suggests that the shearing occurred contemporaneously with the emplacement of the pluton of hornblende-bearing quartz monzonite.

If the trace of the exposed protoclastic border of the hornblende-bearing quartz monzonite were extrapolated southeastward from Grant Lake, it would pass through the glaciated basalt cinder cone north of June Lake and join the arc of the Mono Craters at its south

end. During construction of the Los Angeles Water District tunnel, a large fault zone was found beneath the axis of the Mono Craters (Putnam, 1949, p. 1299). Thus, a rough circle of faults is completed by the arcuate trace of the fault system that no doubt lies beneath the line of Mono Craters eruptive centers and by the fault on the south side of Williams Butte. This circle of faults encloses a topographic low that is the embayment in the east zone of Sierran frontal faults. Inside the circle, all exposed bedrock (though sparse) is hornblende-bearing quartz monzonite.

RANGE-FRONT EMBAYMENT AND THE MONO CRATERS

Russell (1889) concluded that the Mono Craters volcanoes were probably localized along faults related to the faults along the east scarp of the Sierra Nevada. Mayo and others (1936) described the structures in the rhyolite domes south of the Mono Craters and concluded that embayments in the Sierra Nevada scarp in this region are determined by faults in turn controlled by northwest-striking joint sets in the bedrock. They also concluded that north-striking joint sets mark local zones of structural weakness along the east front of the Sierra Nevada, and that one of these zones controls the general trend of the Mono Craters.

The zone of weakness that localized the extrusion of the ryholite domes of the Mono Craters, the andesite dome exposed in the northern part of the Mono Craters chain, and the basalt cinder cone north of June Lake is thought to be the protoclastic border of the hornblende-bearing quartz monzonite, not joint sets or Basin and Range faults, for the following reasons:

1. Exposures of granitic rocks occur on both sides of the south end of the Mono Craters. South of the craters, outcrops of porphyritic quartz monzonite are present; north of the craters, exposures of hornblende-bearing quartz monzonite occur. The buried contact between these granitic plutons is assumedly a zone of protoclasis, for such a zone is exposed at Grant Lake. This zone probably also underlies the axis of the Mono Craters.
2. The trend of the Mono Craters arc and the exposed trace of the contact of the hornblende-bearing quartz monzonite appear to be closely related and to be anomalous to Sierran fault trends.

Surrounding the west half of the circle is a surface of low relief that has an average altitude of 9,000 feet. The surface is mantled by till of Sherwin age and has been deeply dissected by streams and by the ice that flowed across the area during the Tahoe and Tioga Glaciations. Outside the east half of the circle are a ridge capped with volcanic rocks and pumice and the southwest boundary of Mono Lake.

The hornblende-bearing quartz monzonite pluton probably was displaced as a single block during the faulting that caused the present escarpment in this part of the range. Renewed dislocation took place along the contact of the pluton, which had already been sheared during its forceful emplacement, and produced the fractures that are superimposed on the mylonite zone.

Faulting along the ring-fracture zone occurred after the Sherwin Glaciation and before the eruption of the Bishop Tuff. At the south end of Grant Lake and east of June Lake, small outcrops of the Bishop Tuff occur at the same altitude on both sides of the shear zone. Geologic cross sections in the tunnel beneath the Mono Craters (Putnam, 1949), moreover, indicate that there was no displacement of Bishop Tuff across the fault zone beneath the axis of the craters. If any displacement of Bishop Tuff occurred, it took place across the fault beneath the north end of the Mono Craters chain. West of the

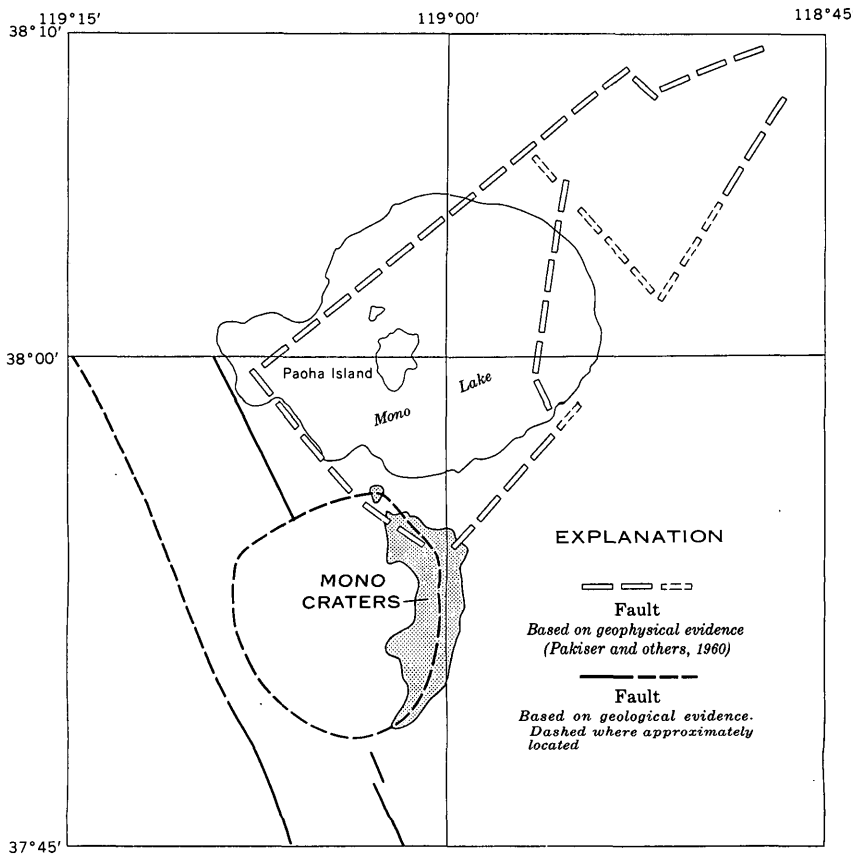

FIGURE 34.—Relation of Mono Craters ring-fracture zone to the geophysically determined subsidence beneath Mono Lake.

ring-fracture zone, however, the surface is mantled with Sherwin Till, offset by the shear zone. An outcrop of Sherwin Till (too small to be shown on the map, fig. 32) is present in the window eroded in Bishop Tuff on the northwest side of Aeolian Buttes.

The geologically determined ring-fracture zone joins the southwest corner of a tectonic depression, as outlined by Pakiser and others (1960), by means of geophysical techniques. The long dimension of the total structure trends northeast, extending about 28 miles (fig. 34).

A residual gravity low of 50 (milligals) over the central part of the basin is interpreted as indicating a subsidence of 18,000 (±5,000) feet resulting from Cenozoic volcanism (Pakiser and others, 1960). This depth of subsidence is based on an assumed density contrast of 0.4g per cc between bedrock and basin fill. If a large amount of pumice were to make up the basin fill, the density contrast would be much greater, and the depth to bedrock required to account for this gravity low would be much less.

A driller's log (R. W. Pack, unpub. data, 1909) for a 2,000-foot-deep hole drilled on Paoha Island indicates that the Bishop Tuff lies 1,350–1,625 feet below the surface of Mono Lake. Using the altitude of Bishop Tuff outcrops on either side of the shear zone north of Reversed Peak as a stationary datum, the prefault surface of the tuff may be projected to Paoha Island along a horizontal line and along a line having a slope of 1.5°; the average slope of undisturbed welded tuff surfaces (Ross and Smith, 1961). This permits the estimate of maximum and minimum displacement of tuff under Mono Lake of approximately 2,800 feet and 1,400 feet, respectively. Calderas and areas of volcano-tectonic subsidence are generally associated with large exposed volumes of welded tuff. No welded tuff older than the Bishop Tuff has been found in the area. Unless older pyroclastic rocks associated with the Mono Basin are found, existing geologic evidence suggests that the geophysical estimate of depth to bedrock beneath Mono Lake may be excessive.

SUMMARY

The area now encompassed by the Mono Craters quadrangle was one of marine sedimentation during most of the Paleozoic. Rocks of Cambrian, Devonian, and Mississippian ages have not been identified and may be absent. The latter hiatus would suggest that the area was structurally high during the Antler orogeny, which affected rocks to the northeast, in Nevada.

Marine miogeosynclinal sedimentary rocks of Paleozoic age, informally termed the "Lewis sequence," were tightly folded along north-striking axial surfaces during a Permian(?) deformation tentatively correlated with the Sonoma orogeny of the same age in Nevada,

as described by Silberling and Roberts (1962). Upper Permian(?) volcanic rocks and clastic sedimentary rocks, now called the Koip sequence, were deposited unconformably on the folded Lewis sequence just after the deformation. Rocks of Triassic age were not identified in the quadrangle.

The Lewis and Koip sequences were folded in a deformation that occured in the Early or Middle Triassic. Axial surfaces of folds formed in this deformation strike northwest and are vertical or steeply dipping. The effects of this deformation are minor east of a zone approximately coincident to the present crest of the Sierra Nevada in this area. A sequence of granodiorite and quartz monzonite plutons was intruded into the Lewis and Koip sequences in the Triassic and Early Jurassic, perhaps during the waning stages of this orogeny.

Coarse clastic sedimentary rocks and volcanic rocks, called the Dana sequence, were deposited in the Early Jurassic. During the subsequent Nevadan orogeny, these and older rocks were deformed. East of a zone approximately coincident to the present crest of the Sierra Nevada, the effects of this deformation were minor.

A pluton of granodiorite, one of a sequence of plutons in the central Sierra Nevada, was intruded into the area of the quadrangle during the Late Cretaceous.

The effects of the deformations determined in the quadrangle have also been noted in the wallrocks and other roof pendants in the Sierra Nevada; thus, they are of regional extent. No correlation could be made between large-scale structures in the intruded pendant rocks and the plutons. Apparently, all the plutonic rocks except the hornblende-bearing quartz monzonite, in the east-central part of the quadrangle, were emplaced passively.

Mineral assemblages in the roof pendants are the result of a complex metamorphic history and are compatible with the hornblende hornfels facies formed by contact metamorphism and the almandine amphibolite facies formed by regional metamorphism.

The Cenozoic history of the quadrangle is one mostly of uplift and erosion, but events that occured prior to Pleistocene glaciation, faulting, and volcanism are not well defined. Most faulting along the front of the Sierra Nevada took place during the Pleistocene, between the Sherwin Glaciation and the eruption of the Bishop Tuff. A maximum of 2,800 feet of fault displacement has occured under Mono Lake since the eruption of the Bishop Tuff.

REFERENCES CITED

Baird, A. K., 1962, Superposed deformations in the central Sierra Nevada foothills east of the Mother Lode: California Univ., Dept. Geol. Sci. Bull., v. 42, no. 1, p. 1–70.

Balk, Robert, 1937, Structural behavior of igneous rocks, with special reference to interpretations by Hans Cloos and collaborators: Geol. Soc. America Mem. 5, 177 p.

Bateman, P. C., 1965, Geology and tungsten mineralization of the Bishop district, California: U.S. Geol. Survey Prof. Paper 470, 208 p.

Bateman, P. C., Clark, L. C., Huber, N. K., Moore, J. G., and Rinehart, C. D., 1963, The Sierra Nevada batholith—a synthesis of recent work across the central part: U.S. Geol. Survey Prof. Paper 414–D, p. D1–D46.

Best, M. G., 1963, Petrology and structural analysis of metamorphic rocks in the southwestern Sierra Nevada foothills, California: California Univ., Dept. Geol. Sci. Bull., v. 42, no. 3, p. 111–158.

Blackwelder, Eliot, 1931, Pleistocene glaciation of the Sierra Nevada and Basin Ranges: Geol. Soc. America Bull., v. 42, no. 4, p. 865–922.

Christensen, M. N., 1963, Structure of metamorphic rocks at Mineral King, California: California Univ., Dept. Geol. Sci. Bull., v. 42, no. 4, p. 159–198.

Clark, L. D., Imlay, R. W., McMath, V. E., and Silberling, N. J., 1962, Angular unconformity between Mesozoic and Paleozoic rocks in the northern Sierra Nevada, California, *in* Short papers in geology, hydrology, and topography: U.S. Geol. Survey Prof. Paper 450–B, p. B15–B19.

Clark, L. D., Stromquist, A. A., and Tatlock, D. B., 1963, Geologic map of the San Andreas quadrangle, Calaveras County, California: U.S. Geol. Survey Geol. Quad. Map GQ–222.

Cloos, Ernst, 1936, Der Sierra-Nevada-Pluton in Californien: Neues Jahrb., supp. vol. 76, no. 3, pt. B., p. 355–450.

Curtis, G. H., Evernden, J. F., and Lipson, J. I., 1958, Age determination of some granitic rocks in California by the potassium-argon method: California Div. Mines Spec. Rept. 54, 16 p.

Dunn, J. R., 1950, Geology of the western Mono Lake area: California Univ., Berkeley, Ph. D. thesis, 130 p.

Evernden, J. F., Curtis, G. H., and Lipson, J. I., 1957, Potassium-argon dating of igneous rocks [California]: Am. Assoc. Petroleum Geologists Bull., v. 41, no. 9, p. 2120–2127.

Ferguson, H. G., and Muller, S. W., 1949, Structural geology of the Hawthorne and Tonopah quadrangles, Nevada: U.S. Geol. Survey Prof. Paper 216, 53 p.

Fyfe, W. S., Turner, F. J., and Verhoogen, Jean, 1958, Metamorphic reactions and metamorphic facies: Geol. Soc. America Mem. 73, 259 p.

Gilbert, C. M., 1938, Welded tuff in eastern California: Geol. Soc. America Bull., v. 49, no. 12, pt. 1, p. 1829–1862.

Huber, N. K., and Rinehart, C. D., 1965, Geologic map of the Devils Postpile quadrangle, Sierra Nevada, California: U.S. Geol. Survey Geol. Quad. Map GQ–437.

Hurley, P. M., Bateman, P. C., Fairbairn, H. W., and Pinson, W. H., Jr., 1965, Investigation of initial Sr^{87}/Sr^{86} ratios in the Sierra Nevada plutonic province: Geol. Soc. America Bull., v. 76, no. 2, p. 165–174.

Kesseli, J. E., 1939, The origin of the valley of June, Gull, and Silver Lakes (horseshoe valley), Mono County, California: Jour. Geology, v. 47, no. 7, p. 748–758.

Kistler, R. W., 1960, The geology of the Mono Craters quadrangle, California: California Univ., Berkeley, Ph. D. thesis, 130 p.

——— 1966, Geologic map of the Mono Craters quadrangle, Mono and Tuolumne Counties, California: U.S. Geol. Survey Geol. Quad. Map GQ–462.

Kistler, R. W., and Bateman, P. C., 1966, Stratigraphy and structure of the Dinkey Creek roof pendant in the central Sierra Nevada, California: U.S. Geol. Survey Prof. Paper, 524–B, 14 p.

Kistler, R. W., Bateman, P. C., and Brannock, W. W., 1965, Isotopic ages of minerals from granitic rocks of the central Sierra Nevada and Inyo Mountains, California: Geol. Soc. America Bull., v. 76, no. 2, p. 155–164.

Kulp, J. L., 1961, Geologic time scale: Science, v. 133, no. 3450, p. 1105–1114.

LeConte, Joseph, 1879, On the extinct volcanoes about Lake Mono and their relation to the glacial drift: Am. Jour. Sci., 3d ser., v. 18, p. 35–44.

Matthes, F. E., 1930, Geologic history of the Yosemite Valley: US. Geol. Survey Prof. Paper 160, 137 p.

Mayo, E. B., 1941, Deformation of the interval Mount Lyell–Mount Whitney, California: Geol. Soc. America Bull., v. 52, no. 7, p. 1001–1084.

Mayo, E. B., Conant, L. C., and Chelikovsky, J. R., 1936, Southern extension of the Mono Craters, California: Am Jour. Sci., 5th ser., v. 32, no. 188, p. 81–97.

McBirney, A. R., and Best, M G, 1961, Experimental deformation of viscous layers in oblique stress fields: Geol. Soc. America Bull., v. 72, p. 495–498.

Moore, J. G., 1963, Geology of the Mount Pinchot quadrangle, southern Sierra Nevada, California: U.S. Geol. Survey Bull. 1130, 152 p.

Pakiser, L. C., Jr., Press, Frank, and Kane, M F., 1960, Geophysical investigation of Mono Basin, California: Geol. Soc. America Bull., v. 71, no. 4, p. 415–447.

Parker, R. B. 1961, Petrology and structural geometry of pre-granitic rocks in the Sierra Nevada, Alpine County, California: Geol. Soc. America Bull., v. 72, no. 12, p. 1789–1806.

Putnam, W. C., 1938, The Mono Craters, California: Geog. Rev., v. 28, no. 1, p. 68–82.

——— 1949, Quaternary geology of the June Lake district, California: Geol. Soc. America Bull., v. 60, no. 8, p. 1281–1302.

Ramsay, J. G., 1958, Superimposed folding at Loch Monar, Inverness-shire and Ross-shire: Geol. Soc. London Quart. Jour., v. 113, p. 271–307.

Rinehart, C D., and Ross, D. C., 1957, Geology of the Casa Diablo Mountain quadrangle, California: U.S. Geol. Survey Geol. Quad Map GQ–99.

——— 1964, Geology and mineral deposits of the Mount Morrison quadrangle, Sierra Nevada, California: U.S. Geol. Survey Prof. Paper 385, 106 p.

Rinehart, C. D., Ross, D. C., and Huber, N. K., 1959, Paleozoic and Mesozoic fossils in a thick stratigraphic section in the eastern Sierra Nevada, California: Geol. Soc. America Bull., v. 70, no. 7, p. 941–945.

Rose, R. L., 1957, Geology of the May Lake area, Yosemite National Park [California]: California Univ., Berkeley, Ph. D. thesis, 219 p.

Ross, C. S., and Smith, R. L., 1961, Ash-flow tuffs—their origin, geologic relations, and identification: U.S. Geol. Survey Prof. Paper 366, 81 p.

Russell, I. C., 1889, Quaternary history of Mono Valley, California: U.S. Geol. Survey 8th Ann. Rept., p. 261–394.

Silberling, N. J., and Roberts, R. J., 1962, Pre-Tertiary stratigraphy and structure of northwestern Nevada: Geol. Soc. America Spec. Paper 72, 58 p.

Tröger, W. E., 1956, Bestimmungstabellen, pt. 1 *of* Optische Bestimmung der gesteinsbildenden Minerale: 2d ed., Stuttgart, E. Schweizerbart'sche Verlagsbuchlandlung, 147 p.

Turner, F. J., 1947, Determination of plagioclase with the four-axis universal stage: Am. Mineralogist, v. 32, nos. 7–8, p. 389–410.

Waters, A. C., and Krauskopf, K. B., 1941, Protoclastic border of the Colville batholith [Washington]: Geol. Soc. America Bull., v. 52, no. 9, p. 1355–1417.

Weiss, L. E., 1959a, Geometry of superposed folding: Geol. Soc. America Bull., v. 70, no. 1, p. 91–106.

——— 1959b, Structural analysis of the basement system at Turoka, Kenya: London, Overseas Geology and Mineral Resources, v. 7, no. 1, p. 3–35; no. 2, p. 123–153.

Whitney, J. D., 1865, Geological Survey of California, Report of progress and synopsis of the field work from 1860 to 1864: California Geol. Survey, Geology, v. 1, 498 p.

Willden, C. R., 1958, Cretaceous and Tertiary orogeny in Jackson Mountains, Humboldt County, Nevada: Am. Assoc. Petroleum Geologists Bull., v. 42, no. 10, p. 2378–2398.

Williams, Howel, 1932, The history and character of volcanic domes: California Univ., Dept. Geol. Sci. Bull., v. 21, no. 5, p. 51–146.

○